Theoretical overview and Global fit

Satoshi Mishima (KEK)

Workshop “Anomalies in b to sll and its implications”
Hongo, University of Tokyo, May 11, 2017

Outline

1. Introduction

   R_K , R_K^* and angular observables in $B \to K^* \mu\mu$

2. Global fits

   model-independent fits of NP contributions

   only R_K , R_K^*

   + angular observables

3. Summary

1. Introduction

- $b \to s\ell^+\ell^-$: FCNC transitions; due to their suppression within the SM, they have a high sensitivity to potential NP contributions.
- In 2013, LHCb [1 fb-1] observed a 3.7 sigma discrepancy between the data and the SM in one bin for P5'.
- In 2015, LHCb [3 fb-1] confirmed it with a 3 sigma deviation in each of two bins.
- LHCb also observed a systematic deficit with respect to the SM predictions for the BRs of several decays, such as $B_s \to \phi\mu\mu$.
- In 2016, Belle confirmed the P5' anomaly.
- Recent ATLAS and CMS data show a good overall agreement with the LHCb results.

$B^0 \to K^{*0}\mu^+\mu^-$

SM:

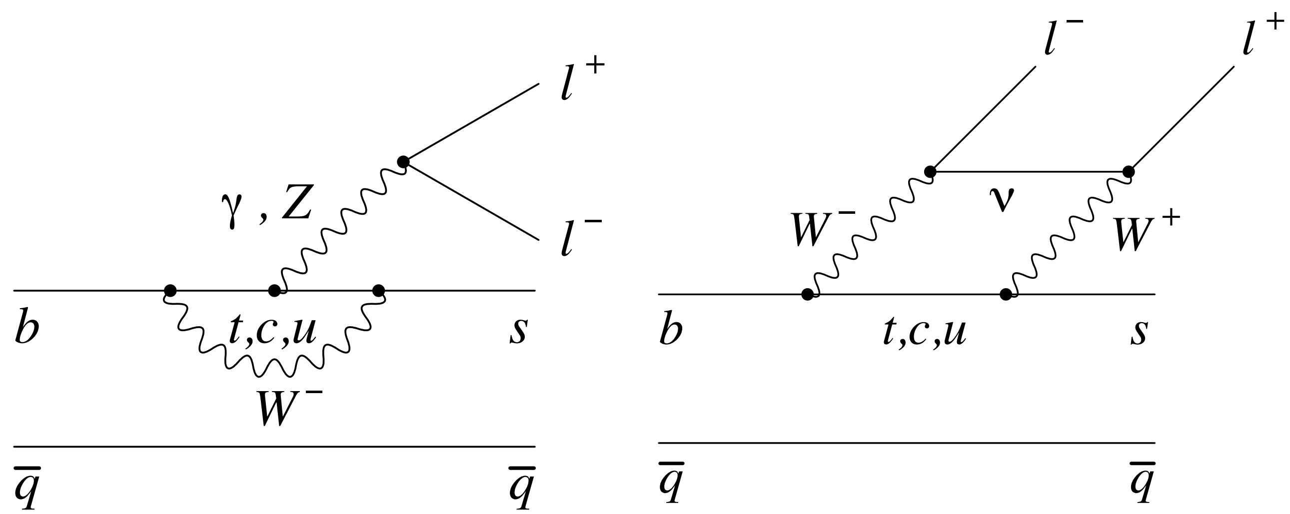

arXiv:0804.4412

EFT:

$$\mathcal{L}_{\rm eff} = \frac{4G_F}{\sqrt{2}} V_{ts} V_{tb}^* \sum_i C_i O_i$$

$$O_9 = \frac{e^2}{16\pi^2}(\bar{b}_L \gamma_\mu s_L)(\bar{\ell}\gamma^\mu \ell)$$

$$O_{10} = \frac{e^2}{16\pi^2}(\bar{b}_L \gamma_\mu s_L)(\bar{\ell}\gamma^\mu \gamma_5 \ell)$$

$$O_{7\gamma} = \frac{e}{16\pi^2} m_b \bar{b}_R \sigma^{\mu\nu} s_L F_{\mu\nu}$$

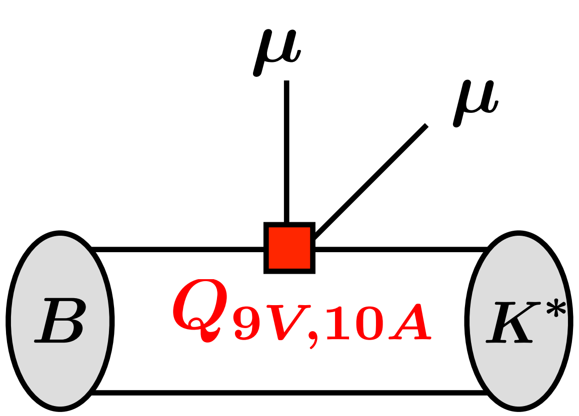

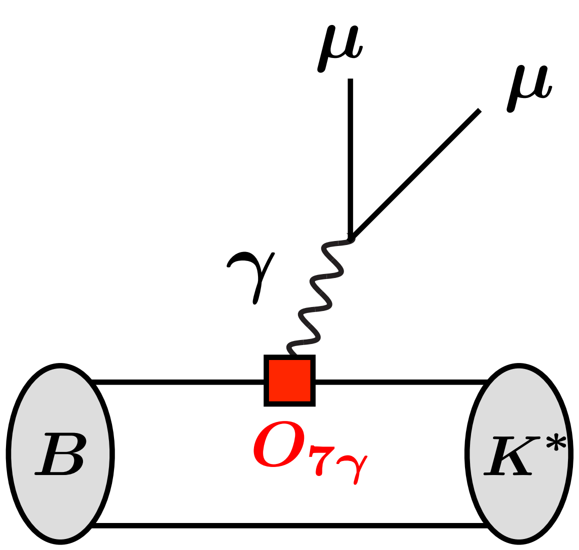

q^2 regions

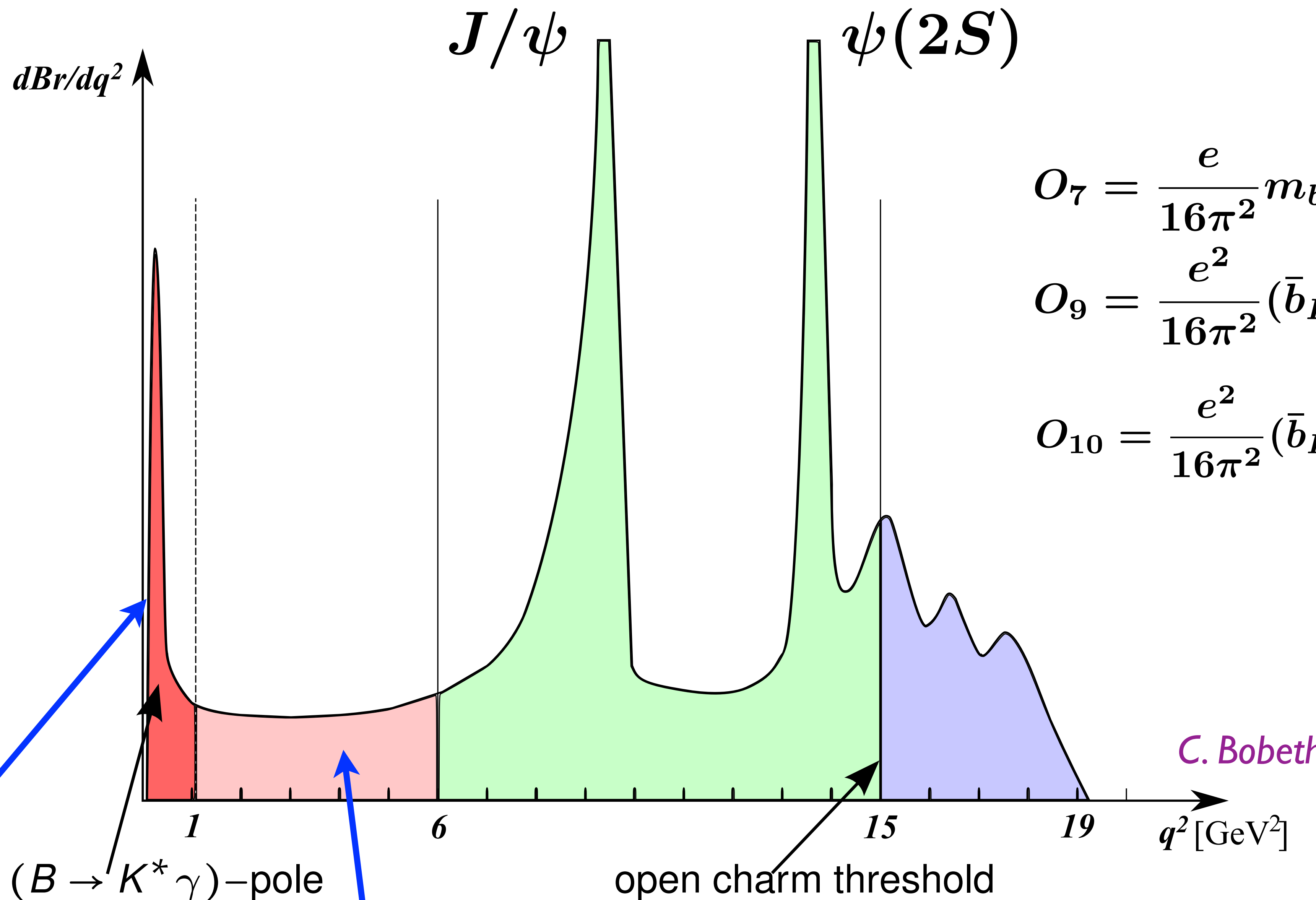

$$O_7 = \frac{e}{16\pi^2} m_b \bar{b}_R \sigma^{\mu\nu} s_L F_{\mu\nu}$$

$$O_9 = \frac{e^2}{16\pi^2} (\bar{b}_L \gamma_\mu s_L)(\bar{\ell}\gamma^\mu \ell)$$

$$O_{10} = \frac{e^2}{16\pi^2} (\bar{b}_L \gamma_\mu s_L)(\bar{\ell}\gamma^\mu \gamma_5 \ell)$$

dominated by O7

dominated by O9

$B \to K^*$ form factors

$$\langle \bar{K}^*(k,\lambda)|\bar{s}\gamma_\mu b|\bar{B}(p)\rangle = \epsilon_{\mu\nu\rho\sigma}\epsilon_\lambda^{*\nu} p^\rho k^\sigma \frac{2}{m_B + m_{K^*}} V(q^2)\,,$$

$$\begin{aligned}\langle \bar{K}^*(k,\lambda)|\bar{s}\gamma_\mu\gamma_5 b|\bar{B}(p)\rangle &= i(\epsilon_\lambda^*\cdot q)\,\frac{2m_{K^*}q_\mu}{q^2}\,A_0(q^2) + i(m_B+m_{K^*})\left(\epsilon^*_{\lambda,\mu} - \frac{(\epsilon_\lambda^*\cdot q)q_\mu}{q^2}\right)A_1(q^2)\\ &\quad - i(\epsilon_\lambda^*\cdot q)\left[\frac{(2p-q)_\mu}{m_B+m_{K^*}} - (m_B - m_{K^*})\,\frac{q_\mu}{q^2}\right]A_2(q^2)\,,\end{aligned}$$

$$q^\nu\langle \bar{K}^*(k,\lambda)|\bar{s}\sigma_{\mu\nu} b|\bar{B}(p)\rangle = 2i\epsilon_{\mu\nu\rho\sigma}\epsilon_\lambda^{*\nu} p^\rho k^\sigma\, T_1(q^2)\,,$$

$$\begin{aligned}q^\nu\langle \bar{K}^*(k,\lambda)|\bar{s}\sigma_{\mu\nu}\gamma_5 b|\bar{B}(p)\rangle &= \left[\epsilon^*_{\lambda,\mu}(m_B^2 - m_{K^*}^2) - (\epsilon^*\cdot q)(2p-q)_\mu\right]T_2(q^2)\\ &\quad + (\epsilon^*\cdot q)\left[q_\mu - \frac{q^2}{m_B^2 - m_{K^*}^2}\,(2p-q)_\mu\right]T_3(q^2)\,,\end{aligned}$$

$$\langle \bar{K}^*(k,\lambda=0)|\bar{s}\gamma_5 b|\bar{B}(p)\rangle = -2i\,\frac{m_{K^*}(\epsilon^*\cdot q)}{m_b+m_s}\,A_0(q^2)$$

- In the heavy quark and low q2 limits,

$$\xi_\perp(q^2) = \frac{m_B}{m_B+m_{K^*}}\,V(q^2) = \frac{m_B+m_{K^*}}{2E}\,A_1(q^2) = T_1(q^2) = \frac{m_B}{2E}\,T_2(q^2)\,,$$

$$\xi_\parallel(q^2) = \frac{m_{K^*}}{E}\,A_0(q^2) = \frac{m_B+m_{K^*}}{2E}\,A_1(q^2) - \frac{m_B-m_{K^*}}{m_B}\,A_2(q^2) = \frac{m_B}{2E}\,T_2(q^2) - T_3(q^2)$$

⇨ only two independent form factors!

$B \to K^*$ form factors

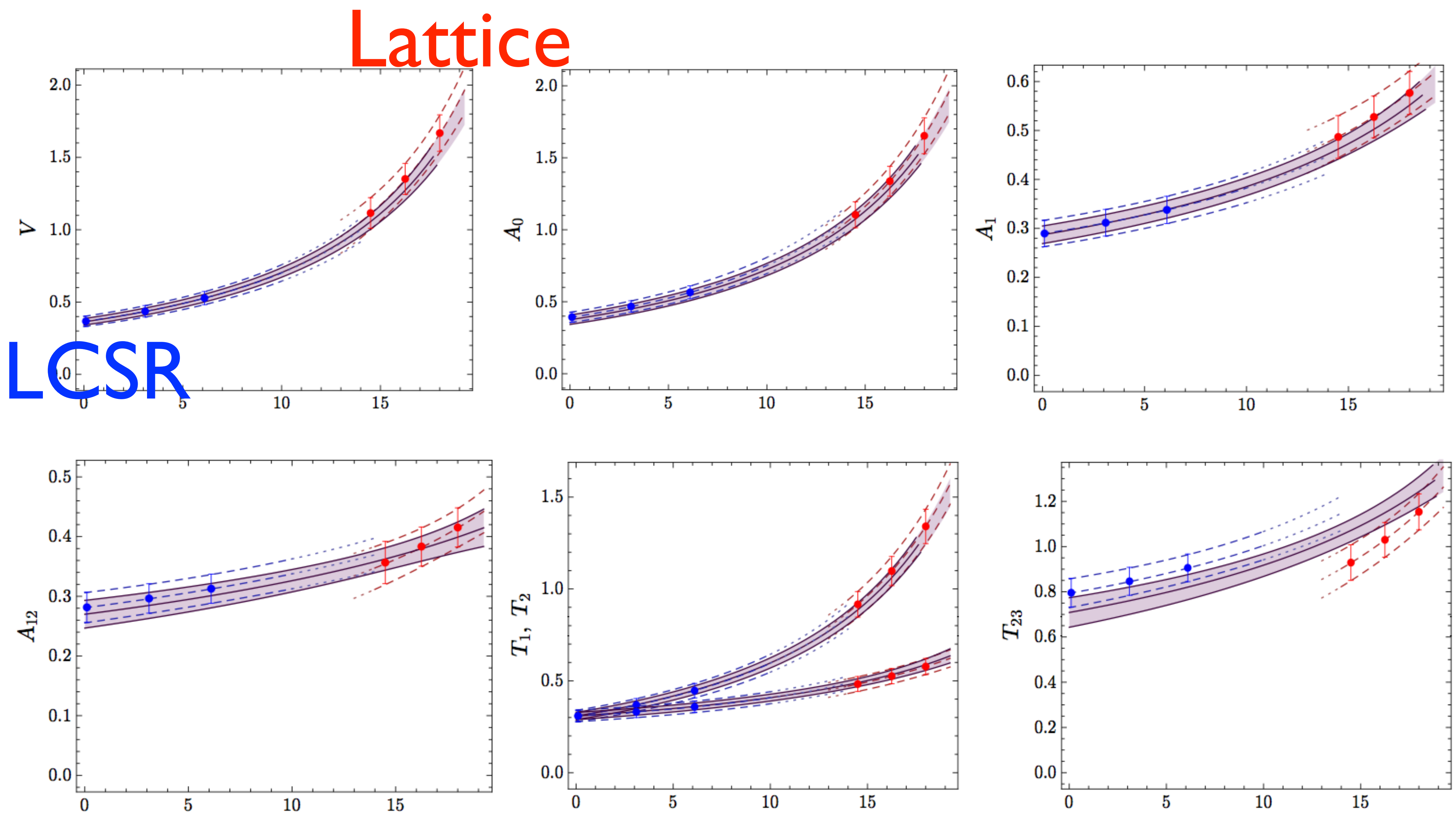

Bharucha, Straub, Zwicky'2015

Optimized angular observables

$$\frac{d^{(4)}\Gamma}{dq^2 d(\cos\theta_\ell) d(\cos\theta_K) d\phi} = \frac{9}{32\pi}\Big(I_1^s \sin^2\theta_K + I_1^c \cos^2\theta_K + (I_2^s \sin^2\theta_K + I_2^c \cos^2\theta_K)\cos 2\theta_\ell$$
$$+ I_3 \sin^2\theta_K \sin^2\theta_\ell \cos 2\phi + I_4 \sin 2\theta_K \sin 2\theta_\ell \cos\phi$$
$$+ I_5 \sin 2\theta_K \sin\theta_\ell \cos\phi + (I_6^s \sin^2\theta_K + I_6^c \cos^2\theta_K)\cos\theta_\ell$$
$$+ I_7 \sin 2\theta_K \sin\theta_\ell \sin\phi + I_8 \sin 2\theta_K \sin 2\theta_\ell \sin\phi$$
$$+ I_9 \sin^2\theta_K \sin^2\theta_\ell \sin 2\phi\Big).$$

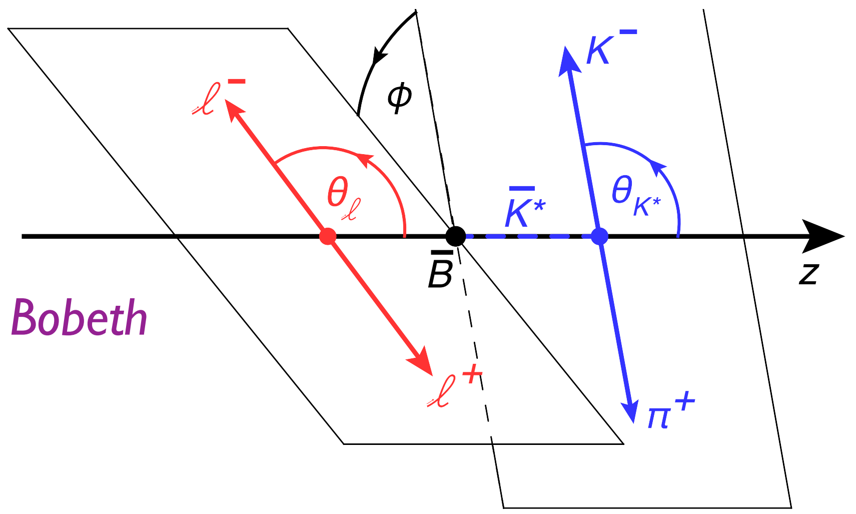

C. Bobeth

$$\Sigma_i \equiv \frac{I_i + \bar{I}_i}{2} = S_i$$

$$P_1 = \frac{\Sigma_3}{2\Sigma_{2s}}, \quad P_2 = \frac{\Sigma_{6s}}{8\Sigma_{2s}}, \quad P_3 = -\frac{\Sigma_9}{4\Sigma_{2s}}, \quad P_4' = \frac{\Sigma_4}{\sqrt{-\Sigma_{2s}\Sigma_{2c}}},$$
$$P_5' = \frac{\Sigma_5}{2\sqrt{-\Sigma_{2s}\Sigma_{2c}}}, \quad P_6' = -\frac{\Sigma_7}{2\sqrt{-\Sigma_{2s}\Sigma_{2c}}}, \quad P_8' = -\frac{\Sigma_8}{\sqrt{-\Sigma_{2s}\Sigma_{2c}}}.$$

Kruger, Matias (05); Egede et al. (08); Descotes-Genon et al. (13)

- less sensitive to form factors

“optimal” in the heavy quark limit ignoring α_s corrections and long-distance hadronic contribution.

Optimized angular observables

$$\boxed{P_1 = \frac{\Sigma_3}{2\Sigma_{2s}}, \quad \Sigma_3 = S_3}$$

$$\Sigma_i \equiv \frac{I_i + \bar{I}_i}{2}$$

- Pi is insensitive to the choice of form factors.

Descotes-Genon et al., 1207.2753

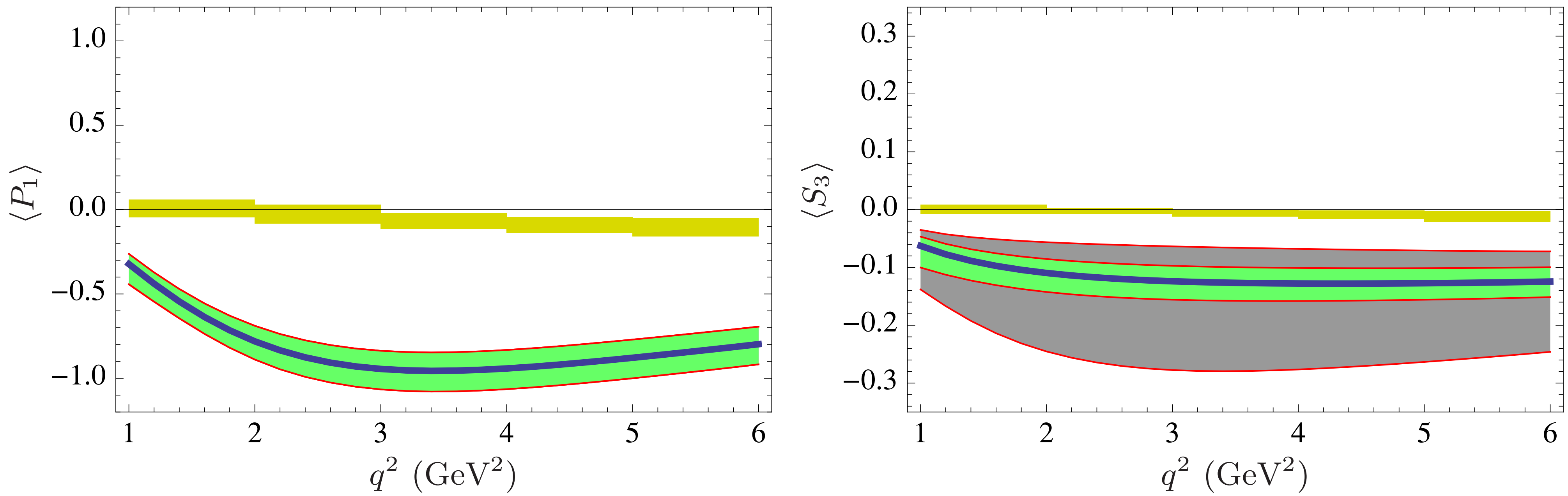

Figure 11. Predictions in the SM and in the case of NP at the benchmark point $b2$ for P_1 (left) and S_3 (right). The yellow boxes are the SM predictions integrated in five 1 GeV^2 bins. The blue curve corresponds to the central values for the NP scenario. The green band is the total uncertainty considering the form factors of refs. [26, 28], while the gray band is the total uncertainty obtained using the form factors of ref. [27]. In the case of P_1 the gray band is barely visible.

Anomaly?

LHCb, 1512.04442

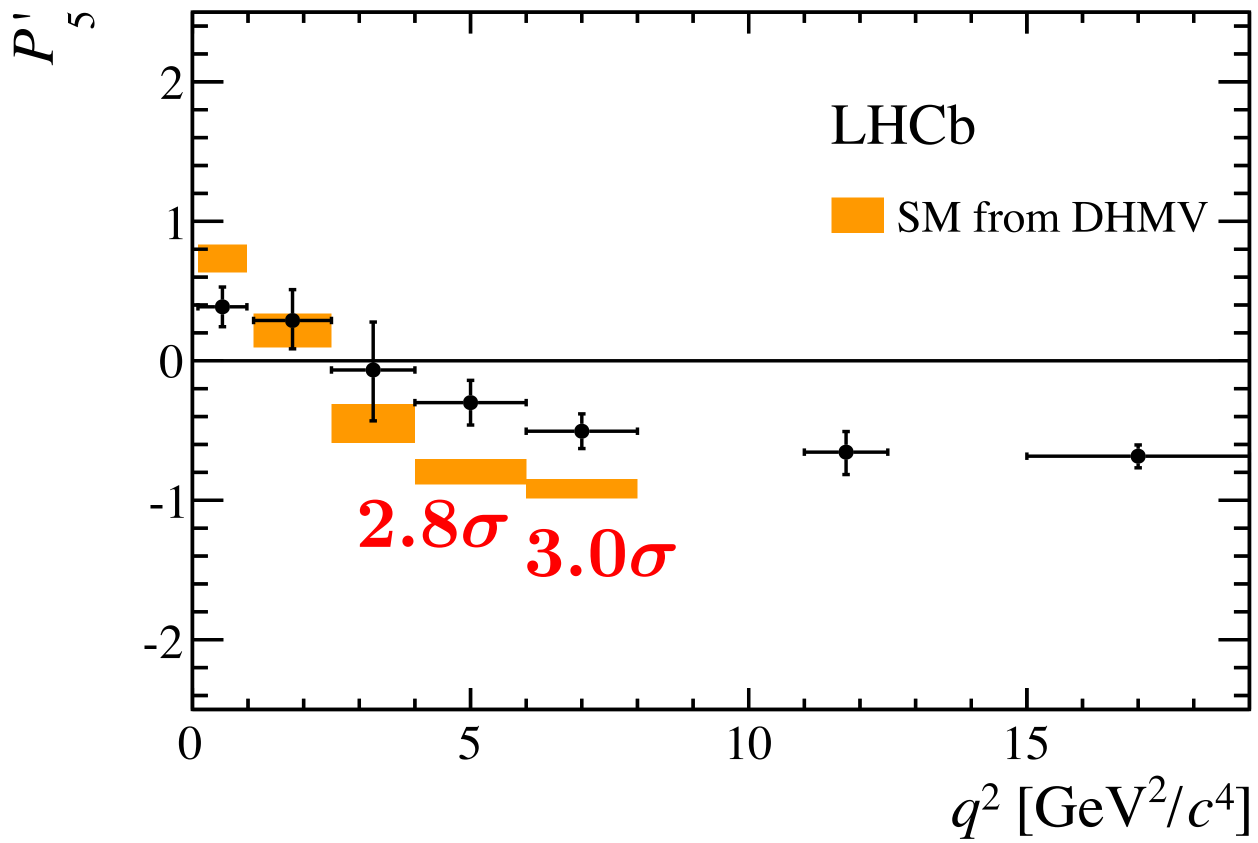

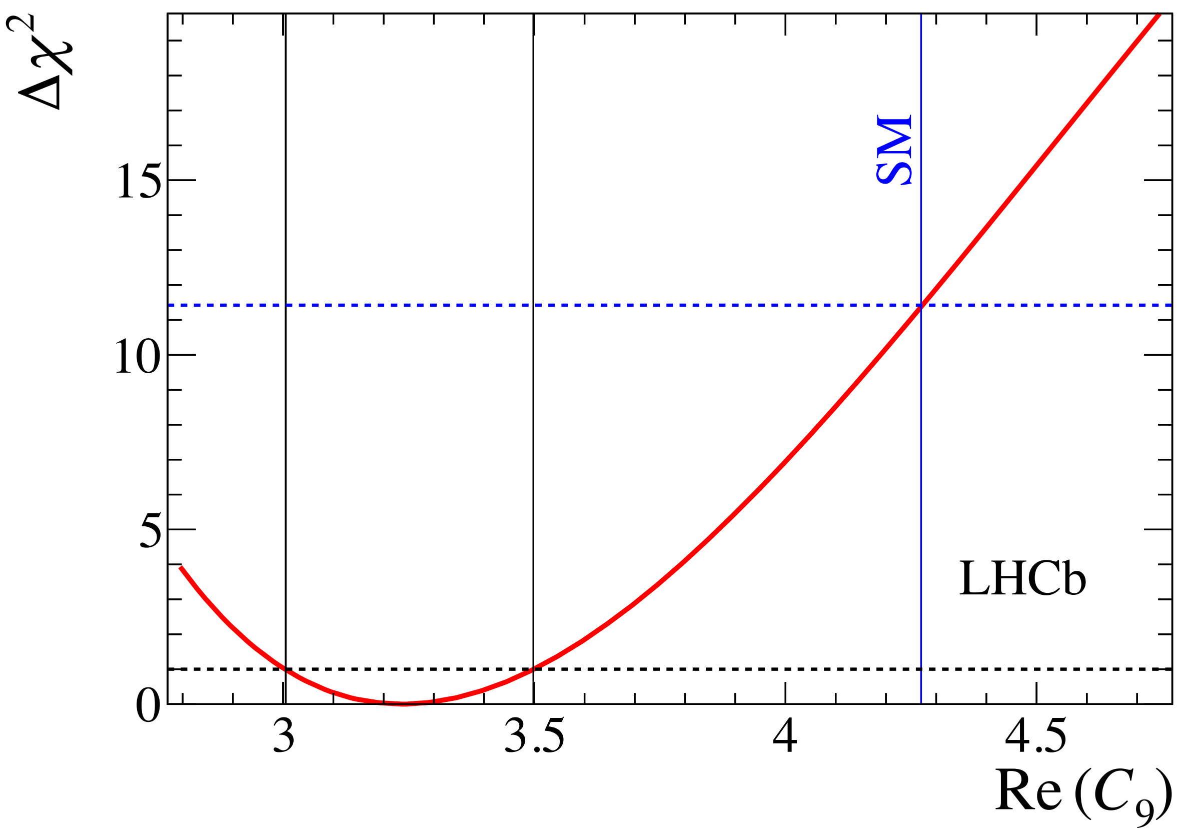

DHMV = Descotes-Genon, Hofer, Matias & Virto (2014)

$$\boxed{C_9^{\rm NP} < 0}$$

$$O_9 = (\bar{s}\gamma_\mu P_L b)(\bar{\ell}\gamma^\mu \ell)$$

$$\left|C_9^{\rm NP}/C_9^{\rm SM}\right| \sim 25\,\%$$

Possible interpretations

$$C_9^{\mathrm{NP}} < 0 \qquad O_9 = (\bar{s}\gamma_\mu P_L b)(\bar{\ell}\gamma^\mu \ell)$$

- NP contribution, e.g., from Z'

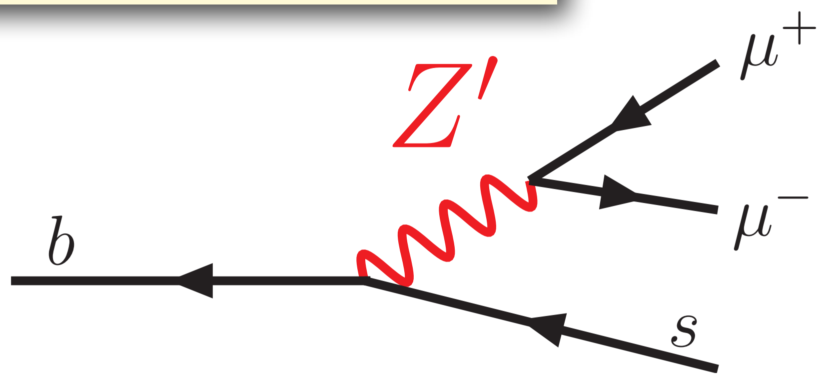

- Hadronic contributions might mimic a short distance NP contribution in $C_{9\mu}$.

  Underestimate of SM uncertainty from long-distance charm loops ?

$$O_2 = (\bar{b}\gamma_\mu P_L c)(\bar{c}\gamma^\mu P_L s)$$

LCSR estimate *Khodjamirian et al. (2010)*

Main problem for the P5' anomaly!!

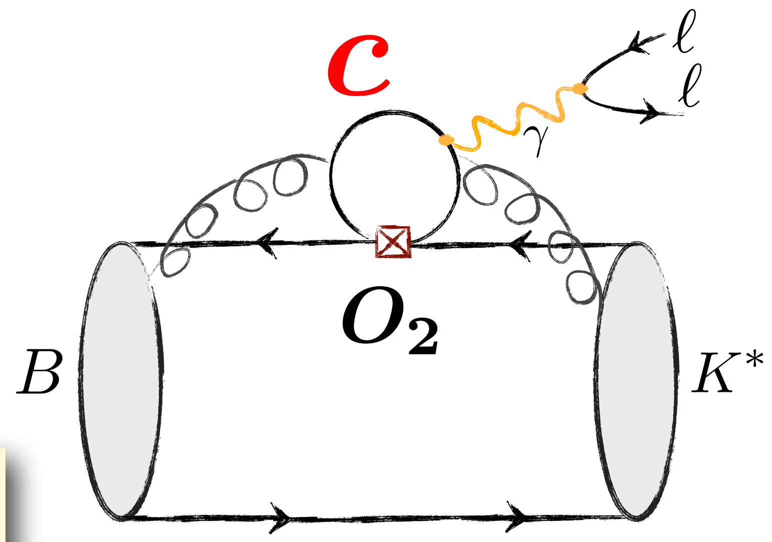

P5' anomaly in $B \to K^* \mu^+ \mu^-$

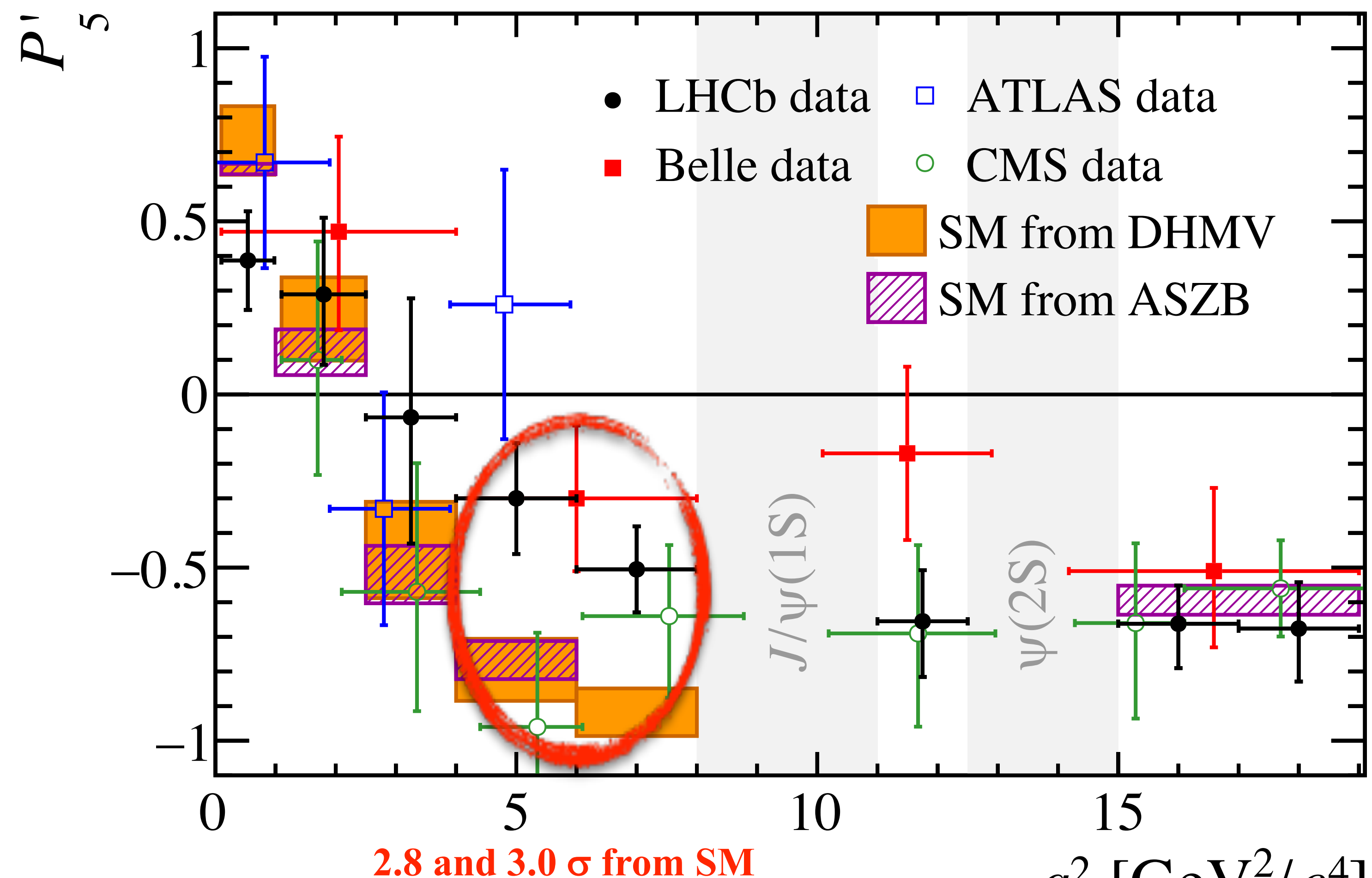

- JHEP 02 (2016) 104
- PRL 118 (2017)
- ATLAS-CONF-2017-023
- CMS-PAS-BPH-15-008

- DHMV vs. ASZB:

  different inputs for form factors

  different parameterizations of hadronic contributions and power-suppressed contributions

LFU ratios $R_{K^{(*)}}$

- The Lepton Flavor Universality (LFU) ratios are very clean probes of NP:

$$R_M[q^2_{\rm min},\, q^2_{\rm max}] = \frac{\displaystyle\int_{q^2_{\rm min}}^{q^2_{\rm max}} dq^2 \frac{d\Gamma(B \to M\mu^+\mu^-)}{dq^2}}{\displaystyle\int_{q^2_{\rm min}}^{q^2_{\rm max}} dq^2 \frac{d\Gamma(B \to M e^+ e^-)}{dq^2}}$$

- very clean theoretically; hadronic uncertainties cancel to large extent in the ratio. *Hiller & Kruger, hep-ph/0310219*

- potential to discriminate among NP models.

Hiller & Schmaltz, 1411.4773

- The SM values of $R_{K^{(*)}}$ are expected to deviate from unity only at the percent level, considering QED logarithmic corrections. *Bordone, Isidori & Pattori, 1605.07633*

LHCb data for $R_{K^{(*)}}$

$$R_K^{[1,6]} = 0.745^{+0.090}_{-0.074} \pm 0.036$$ 2.6 sigma

$$R_{K^*}^{[0.045,1.1]} = 0.660^{+0.110}_{-0.070} \pm 0.024$$ ~2.4 sigma

$$R_{K^*}^{[1.1,6]} = 0.685^{+0.113}_{-0.069} \pm 0.047$$ ~2.5 sigma

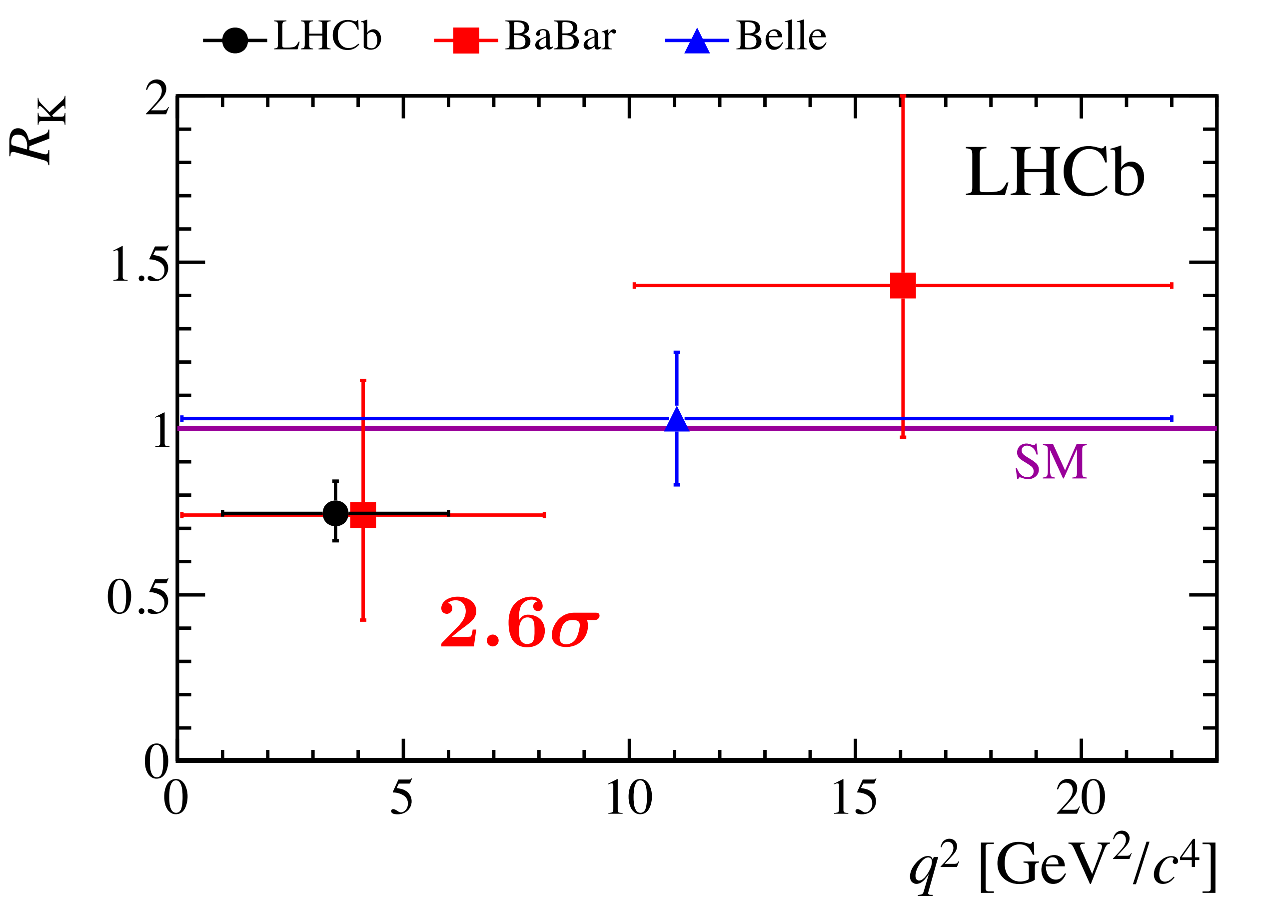

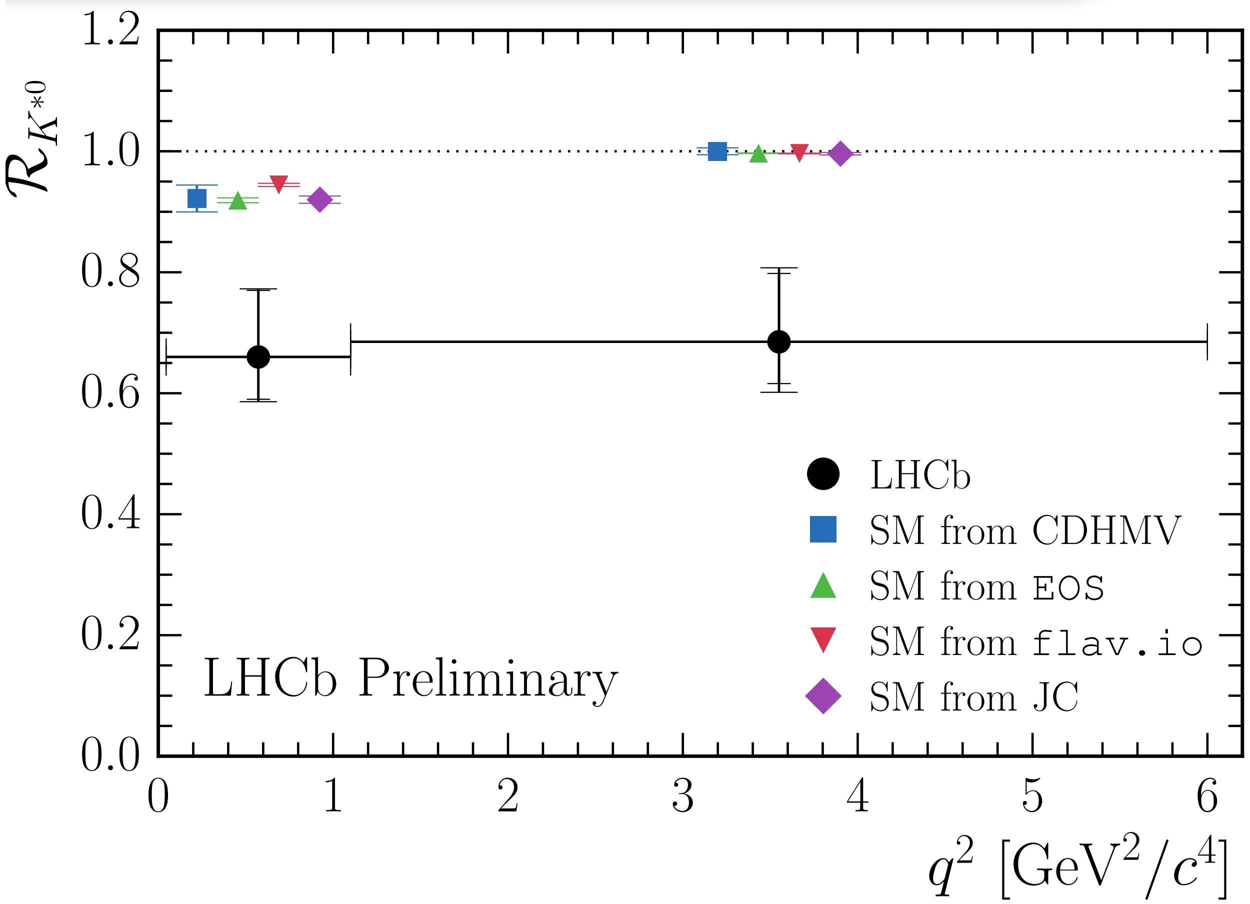

Sources of LFU violation in the SM

- masses of the charged leptons

  relevant only for a very small di-lepton invariant mass squared close to $q^2 \sim 4m_\ell^2$

- their interactions with the Higgs
- (negligibly small neutrino masses)

  ➡ tiny effects in rare B decays

- Hadronic contributions cannot generate LFU violation.

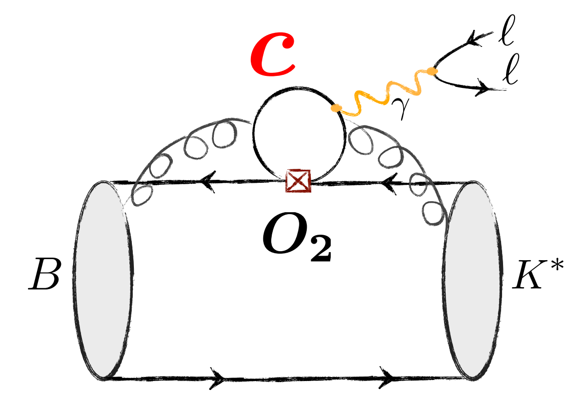

LFUV data from Belle

Belle, 1612.05014

- Belle reported data for LFUV observables, but not yet statistically significant.

$$Q_{4,5} = P'^{\mu}_{4,5} - P'^{e}_{4,5}$$

$$\mathrm{NP}: C^{\mathrm{NP}}_{9\mu} = -1.1$$

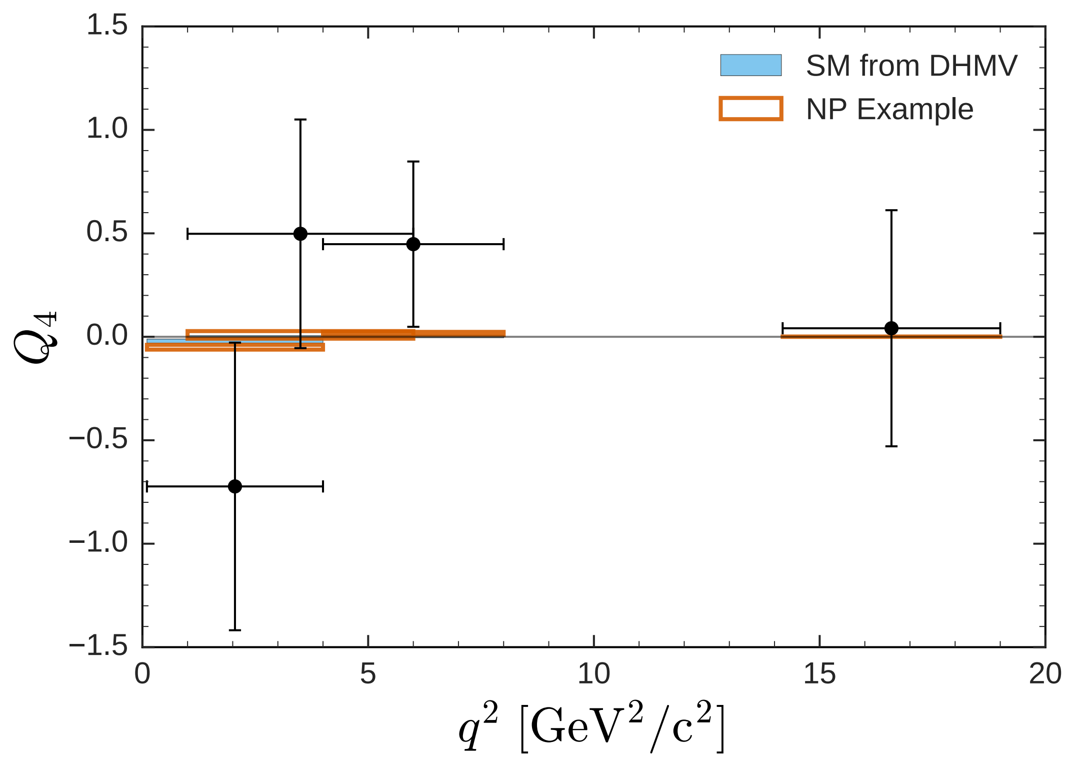

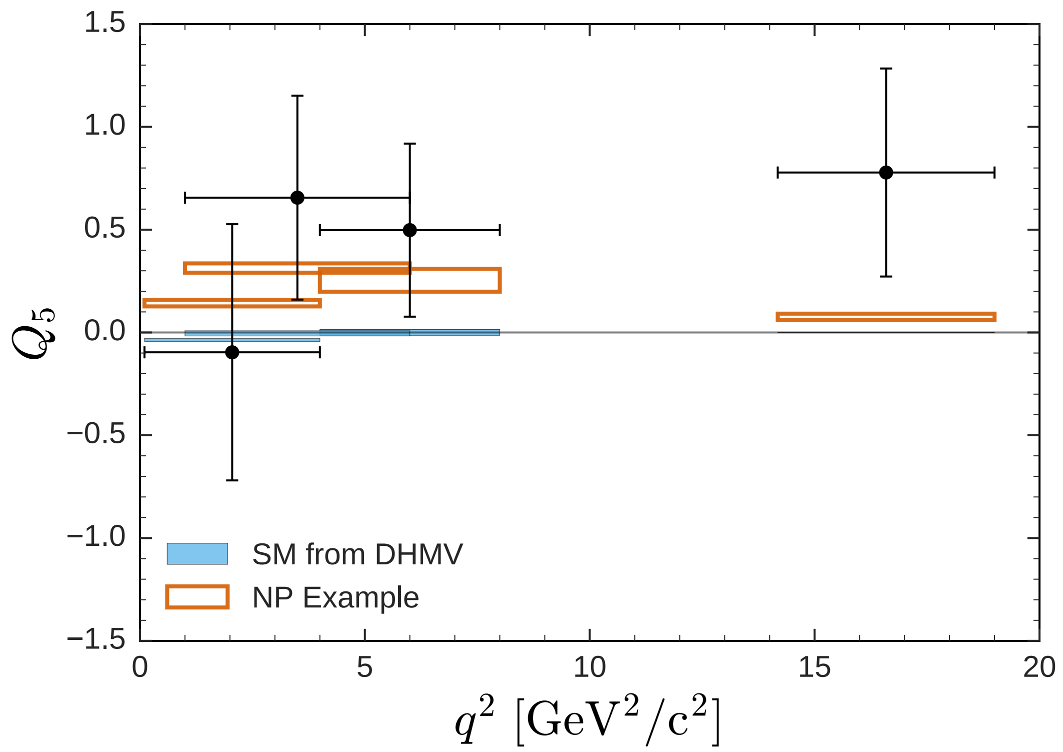

- Less sensitive to hadronic contributions.

Clean or Dirty

- LFUV observables $R_{K^{(*)}}$ and $Q_{4,5} = P'^{\mu}_{4,5} - P'^{e}_{4,5}$

  less sensitive to hadronic contributions

  theoretically clean!

- Angular observables, such as P5'

  suffer from hadronic contributions

  dirty!

2. Global fits

Relevant operators

$$\mathcal{H}_{\text{eff}} = -\frac{4G_F}{\sqrt{2}} V_{tb} V_{ts}^* \frac{\alpha}{4\pi} \sum_i C_i^\ell \mathcal{O}_i^\ell + \text{h.c.},$$

$$\mathcal{O}_9^\ell = (\bar{s}\gamma^\mu P_L b)(\bar{\ell}\gamma_\mu \ell), \quad \mathcal{O}_9'^\ell = (\bar{s}\gamma^\mu P_R b)(\bar{\ell}\gamma_\mu \ell),$$

$$\mathcal{O}_{10}^\ell = (\bar{s}\gamma^\mu P_L b)(\bar{\ell}\gamma_\mu \gamma_5 \ell), \quad \mathcal{O}_{10}'^\ell = (\bar{s}\gamma^\mu P_R b)(\bar{\ell}\gamma_\mu \gamma_5 \ell),$$

chirality flipped

- In the SM,

$$C_9(\mu_b) \approx 4.1 \qquad C_9'(\mu_b) \approx 0$$

$$C_{10}(\mu_b) \approx -4.2 \qquad C_{10}'(\mu_b) \approx 0$$

- Operators with chiral lepton currents:

$$\mathcal{O}_{AB}^\ell = (\bar{s}\gamma^\mu P_A b)(\bar{\ell}\gamma_\mu P_B \ell)\,, \qquad A, B = L, R$$

$$\Rightarrow \quad C_{LL}^{\text{SM}} = C_9^{\text{SM}} - C_{10}^{\text{SM}} \approx 8.4$$

Patterns of NP in $R_{K^{(*)}}$

- The dipole operator $O_{7\gamma}$ and four-quark operators cannot lead to LFUV.
- The (pseudo-)scalar operators are strongly constrained by $B(B_s \to \ell\ell)$.

Alonso, Grinstein & Martin Camalich, 1407.7044
Altmannshofer, Niehoff & Straub, 1702.05498

- NP in $C_9^{(\prime)\mu}$ and $C_{10}^{(\prime)\mu}$

The nodes indicate steps of $\Delta C_i^\mu = +0.5$.

$$R_K \not\approx R_{K^*}$$

⇩

the presence of chirality flipped contributions

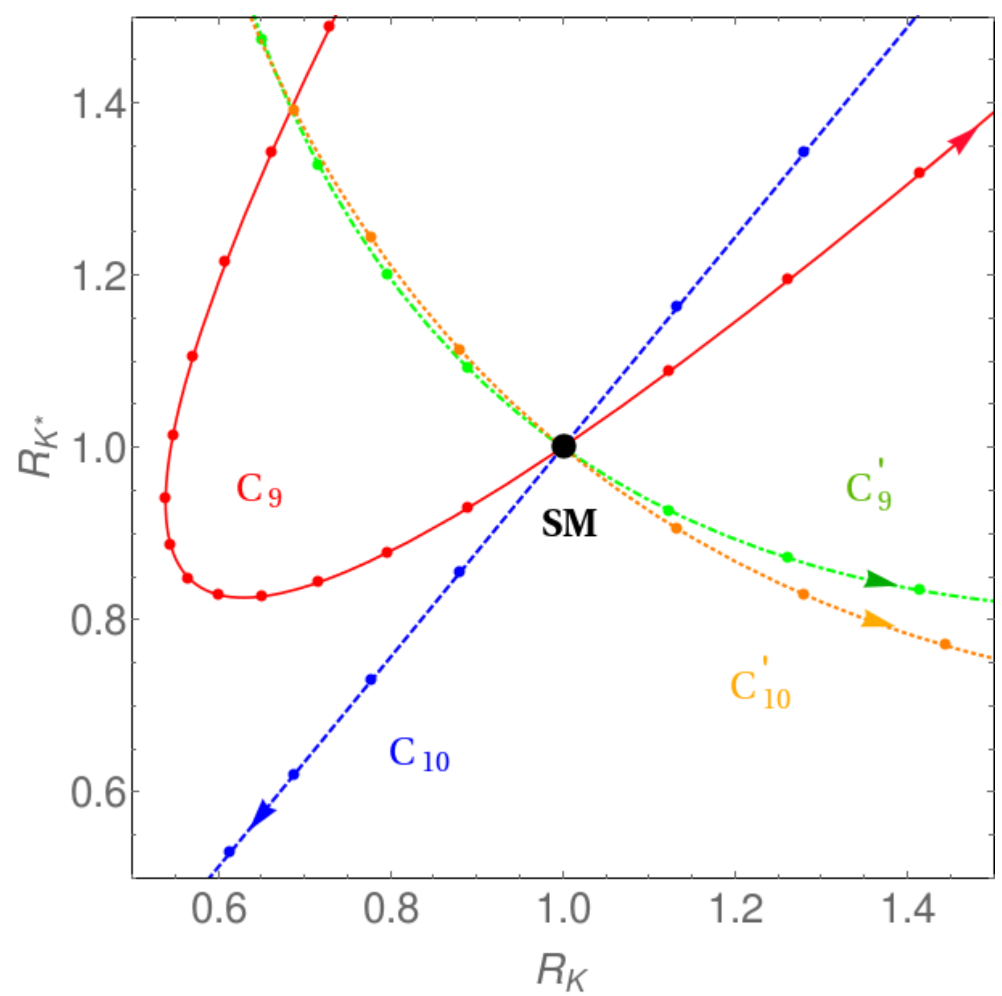

Geng, Grinstein, Jager, Martin Camalich, Ren & Shi, 1704.05446

Patterns of NP in $R_{K^{(*)}}$

- $B \to K\ell\ell$

$$\frac{d\Gamma_K}{dq^2} = \mathcal{N}_K |\vec{k}|^3 f_+(q^2)^2 \left(|C_{10}^\ell + C_{10}'^\ell|^2 + \left| C_9^\ell + C_9'^\ell + 2\frac{m_b}{m_B + m_K} C_7 \frac{f_T(q^2)}{f_+(q^2)} - 8\pi^2 h_K \right|^2 \right) + \mathcal{O}(\frac{m_\ell^4}{q^4}) + \frac{m_\ell^2}{m_B^2} \times O(\alpha_s, \frac{q^2}{m_B^2} \times \frac{\Lambda}{m_b}),$$

f_i, V_i, T_i : form factors
h_i : hadronic contributions

- $B \to K^*\ell\ell$ $\quad \frac{d\Gamma_{\bar{K}^*}}{dq^2} = \frac{d\Gamma_\perp}{dq^2} + \frac{d\Gamma_0}{dq^2}$

$$\frac{d\Gamma_0}{dq^2} = \mathcal{N}_{K^*0} |\vec{k}|^3 V_0(q^2)^2 \left(|C_{10}^\ell - C_{10}'^\ell|^2 + \left| C_9^\ell - C_9'^\ell + \frac{2m_b}{m_B} C_7 \frac{T_0(q^2)}{V_0(q^2)} - 8\pi^2 h_{K^*0} \right|^2 \right) + \mathcal{O}\left(\frac{m_\ell^2}{q^2}\right),$$

$$\frac{d\Gamma_\perp}{dq^2} = \mathcal{N}_{K^*\perp} |\vec{k}| q^2 V_-(q^2)^2 \left(|C_{10}^\ell|^2 + |C_9'^\ell|^2 + |C_{10}'^\ell|^2 + \left| C_9^\ell + \frac{2m_b m_B}{q^2} C_7 \frac{T_-(q^2)}{V_-(q^2)} - 8\pi^2 h_{K^*\perp} \right|^2 \right) + \mathcal{O}\left(\frac{m_\ell^2}{q^2}\right) + \mathcal{O}\left(\frac{\Lambda}{m_b}\right)$$

- $V_+(q^2)$ and $T_+(q^2)$ are power suppressed.

$A_0 : A_- : A_+ = 1 : \Lambda/m_b : \Lambda^2/m_b^2$ in the heavy quark limit

- relative minus signs due to the different parities.
- Chirality flipped contributions increase the decay rate in the transverse polarization.

Fit of $R_{K^{(*)}}$

- NP in muon couplings: *Geng, Grinstein, Jager, Martin Camalich, Ren & Shi, 1704.05446*

$R_{K^{(*)}}$ only

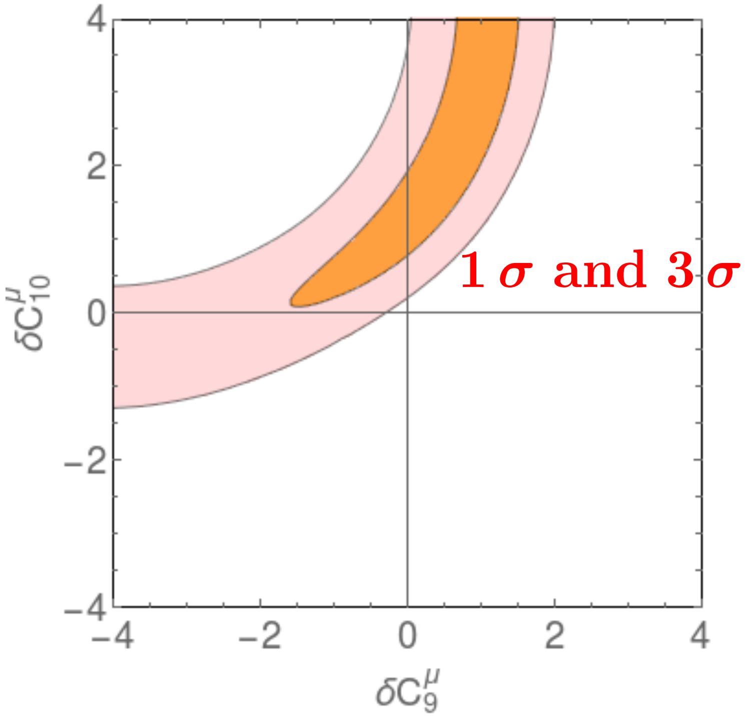

$+B(B_s \to \mu\mu)$

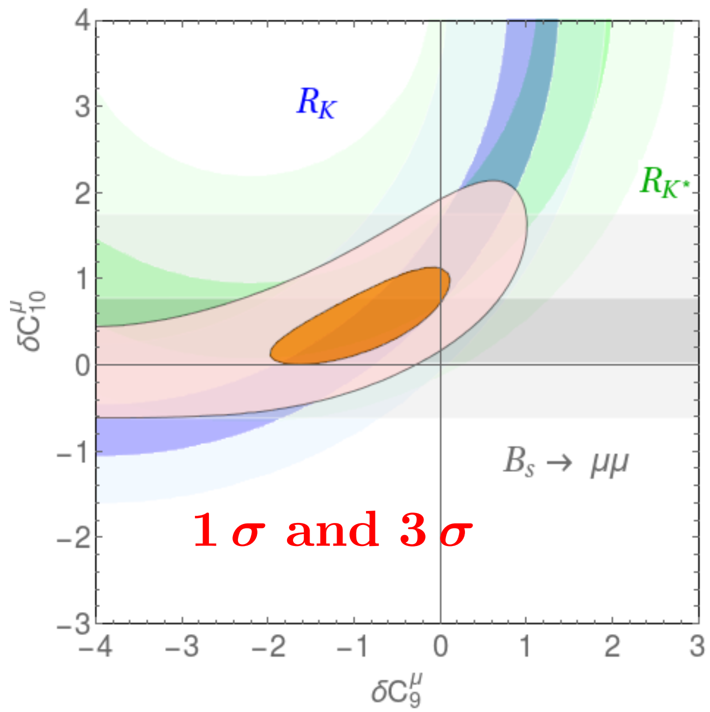

- The fit favors NP in the directions of $\delta C_9^\mu = -\delta C_{10}^\mu$.
- NP in electron couplings produces very similar results with $\delta C_i^e \approx -\delta C_i^\mu$.

Fit results

Coeff.	best fit	1σ	2σ	pull
C_9^μ	-1.59	$[-2.15, -1.13]$	$[-2.90, -0.73]$	4.2σ
C_{10}^μ	$+1.23$	$[+0.90, +1.60]$	$[+0.60, +2.04]$	4.3σ
C_9^e	$+1.58$	$[+1.17, +2.03]$	$[+0.79, +2.53]$	4.4σ
C_{10}^e	-1.30	$[-1.68, -0.95]$	$[-2.12, -0.64]$	4.4σ
$C_9^\mu = -C_{10}^\mu$	-0.64	$[-0.81, -0.48]$	$[-1.00, -0.32]$	4.2σ
$C_9^e = -C_{10}^e$	$+0.78$	$[+0.56, +1.02]$	$[+0.37, +1.31]$	4.3σ
$C_9'^\mu$	-0.00	$[-0.26, +0.25]$	$[-0.52, +0.51]$	0.0σ
$C_{10}'^\mu$	$+0.02$	$[-0.22, +0.26]$	$[-0.45, +0.49]$	0.1σ
$C_9'^e$	$+0.01$	$[-0.27, +0.31]$	$[-0.55, +0.62]$	0.0σ
$C_{10}'^e$	-0.03	$[-0.28, +0.22]$	$[-0.55, +0.46]$	0.1σ

Altmannshofer, Stangl & Straub, 1704.05435

- A good description of the data is given by

$$C_9^\mu - C_9^e - C_{10}^\mu + C_{10}^e \simeq -1.4$$

unless some of the individual coefficients are much larger than one in absolute value.

Chirality-flipped operators

- The primed coefficients, corresponding to right-handed quark currents, cannot improve the agreement with the data by themselves.

$$\mathcal{O}_9'^{\ell} = (\bar{s}\gamma^\mu P_R b)(\bar{\ell}\gamma_\mu \ell), \quad \mathcal{O}_{10}'^{\ell} = (\bar{s}\gamma^\mu P_R b)(\bar{\ell}\gamma_\mu \gamma_5 \ell)$$

$$R_{K^*} > 1, \; R_K < 1$$

and vice versa

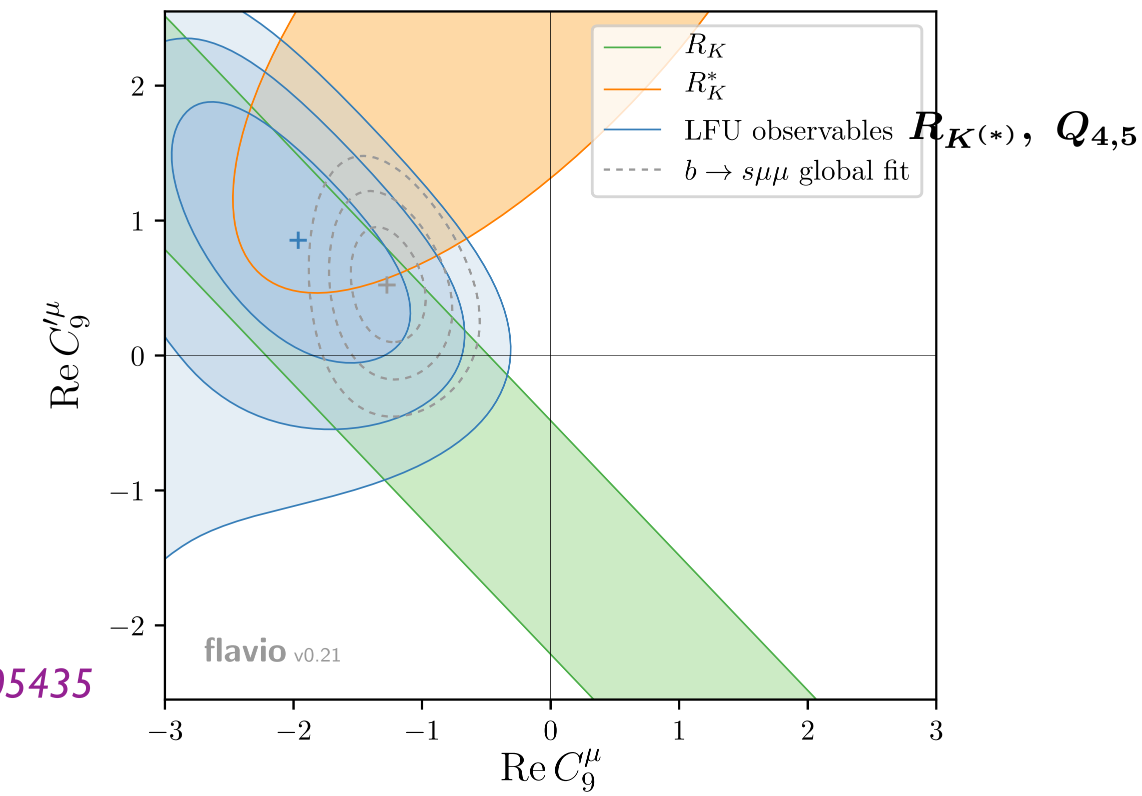

Altmannshofer, Stangl & Straub, 1704.05435

- In combination with sizable un-primed coefficients, the primed coefficients can slightly improve the fit.

Chiral lepton currents

$$\mathcal{O}^{\ell}_{AB} = (\bar{s}\gamma^{\mu} P_A b)(\bar{\ell}\gamma_{\mu} P_B \ell)\,, \qquad A, B = L, R$$

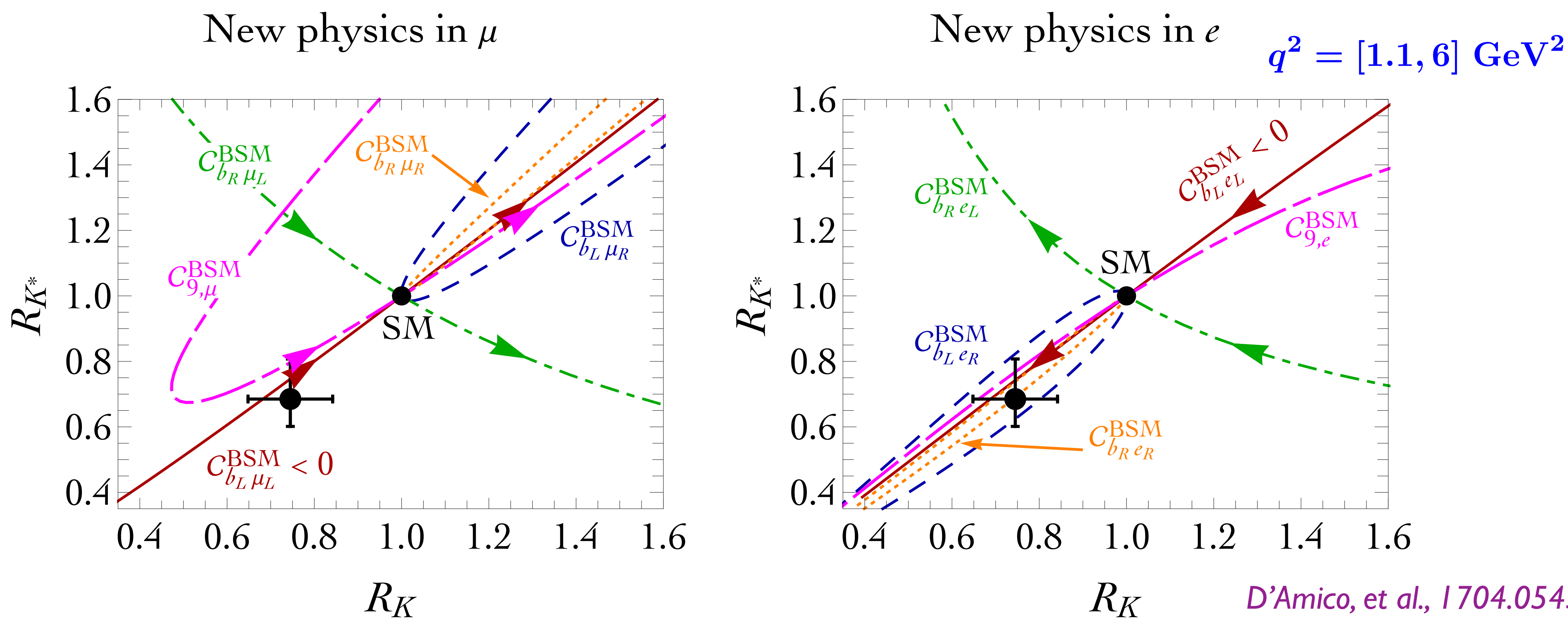

D'Amico, et al., 1704.05438

- A reduction of the same order in both ratios is possible in the presence of negative $C^{\rm BSM}_{b_L\mu_L}$.
- $R_{K^{(*)}} < 1$ ⇨ $b_L\mu_L,\ b_L e_L,\ b_L e_R,\ b_R e_R$

q2 dependence

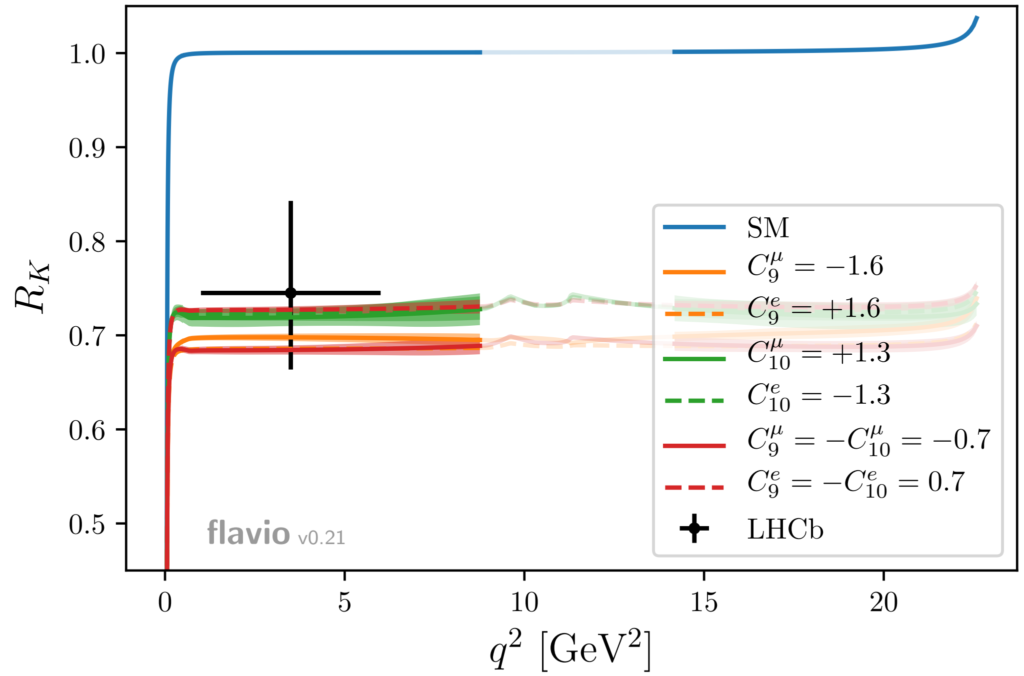

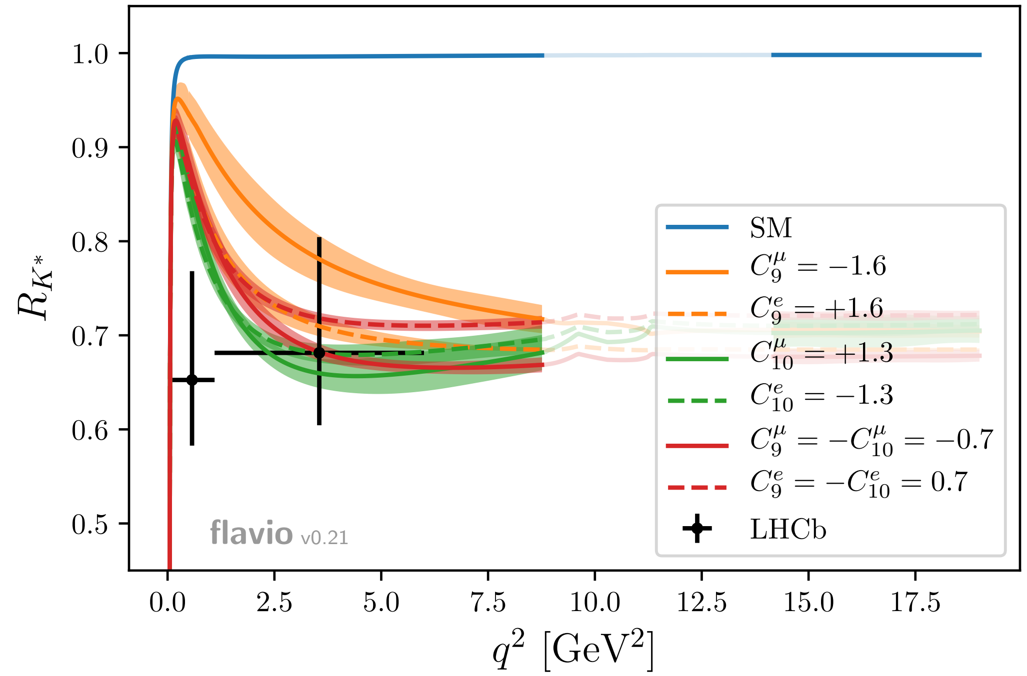

$$C_9^\ell \Rightarrow R_K \lesssim R_{K^*} < 1$$

$$C_{10}^\ell \Rightarrow R_{K^*} \lesssim R_K < 1$$

Altmannshofer, Stangl & Straub, 1704.05435

- In the SM, uncertainties almost cancel in the ratio, but it's no longer true in presence of lepton-specific NP contributions.

- R_{K^*} at low q2 is dominated by the photon pole, which gives a LFU contribution.

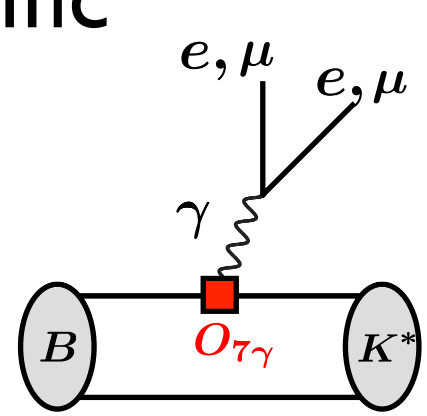

First bin of R_{K^*}

- The first bin is dominated by the dipole operator, which is bounded by $B(B \to X_s\gamma)$.
- It is difficult to accommodate the data for the first bin through C9 and C10.
- A significant discrepancy in the first bin would imply the existence of light NP degrees of freedom.
- More precise measurements will be important to clarify this issue.

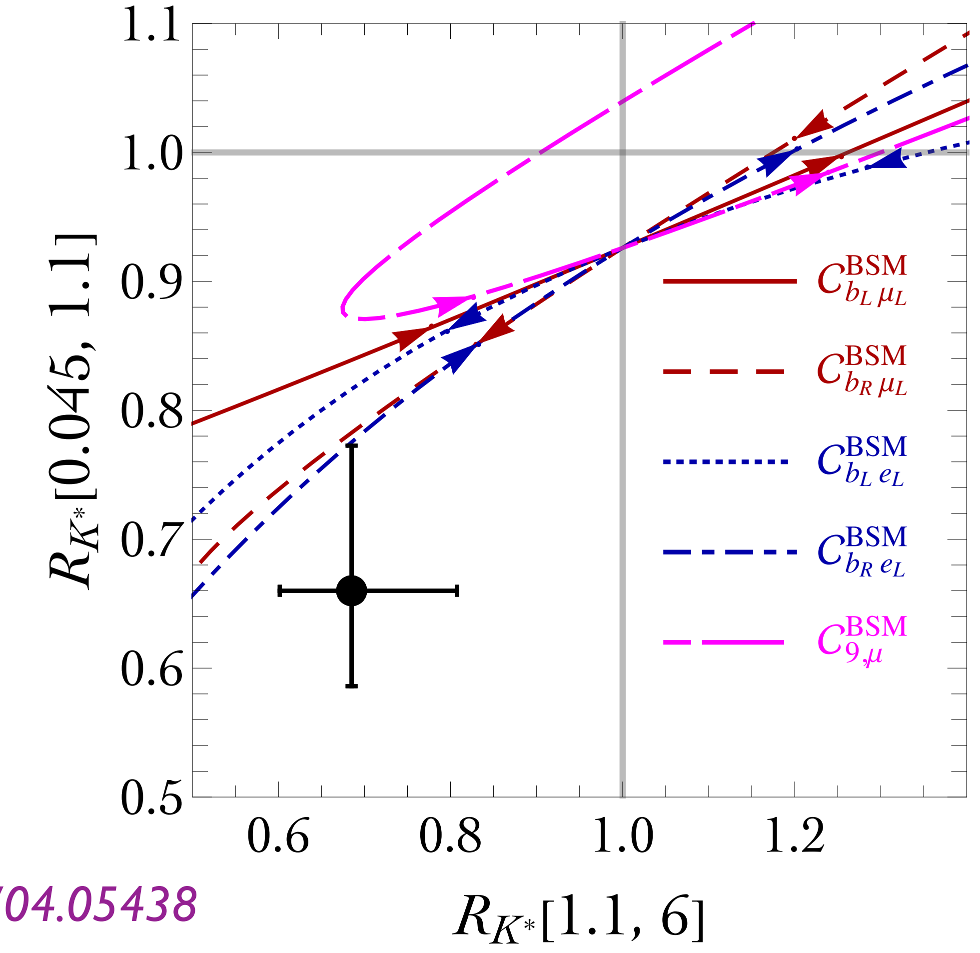

D'Amico, et al., 1704.05438

Global fit

Capdevila, Crivellin, Descotes-Genon, Matias & Virto, 1704.05340

- Two cases:
  - LFUV(17measurements): $R_{K^{(*)}}\,(\mathrm{LHCb}),\ Q_{4,5}\,(\mathrm{Belle})$
  - All (175): $B\to K^*\mu\mu\,(\mathrm{ATLAS, Belle, CMS, LHCb})$ + above
    $B_s\to\phi\mu\mu\,(\mathrm{LHCb})$

  $B(B\to X_s\gamma),\ B(B\to X_s\mu\mu),\ B(B_s\to\mu\mu),$ etc. are also included in both cases.

- Main anomalies:

Largest pulls	$\langle P_5'\rangle_{[4,6]}$	$\langle P_5'\rangle_{[6,8]}$	$R_K^{[1,6]}$	$R_{K^*}^{[0.045,1.1]}$	$R_{K^*}^{[1.1,6]}$	$\mathcal{B}^{[2,5]}_{B_s\to\phi\mu^+\mu^-}$	$\mathcal{B}^{[5,8]}_{B_s\to\phi\mu^+\mu^-}$
Experiment	-0.30 ± 0.16	-0.51 ± 0.12	$0.745^{+0.097}_{-0.082}$	$0.66^{+0.113}_{-0.074}$	$0.685^{+0.122}_{-0.083}$	0.77 ± 0.14	0.96 ± 0.15
SM prediction	-0.82 ± 0.08	-0.94 ± 0.08	1.00 ± 0.01	0.92 ± 0.02	1.00 ± 0.01	1.55 ± 0.33	1.88 ± 0.39
Pull (σ)	-2.9	-2.9	+2.6	+2.3	+2.6	+2.2	+2.2
Prediction for $\mathcal{C}_{9\mu}^{\rm NP}=-1.1$	-0.50 ± 0.11	-0.73 ± 0.12	0.79 ± 0.01	0.90 ± 0.05	0.87 ± 0.08	1.30 ± 0.26	1.51 ± 0.30
Pull (σ)	-1.0	-1.3	+0.4	+1.9	+1.2	+1.8	+1.6

- SM: p=4.4% for LFUV and p=14.6% for All

Satoshi Mishima (KEK)

Global fit w/o LFUV observables

Altmanshofer, Niehoff, Stangl & Straub, 1703.09189

- NP in $b \to s\mu\mu$

Coeff.	best fit	1σ	2σ	pull
$C_9^{\rm NP}$	-1.19	$[-1.41, -0.97]$	$[-1.61, -0.73]$	4.9σ
C_9'	$+0.13$	$[-0.08, +0.34]$	$[-0.29, +0.55]$	0.6σ
$C_{10}^{\rm NP}$	$+0.64$	$[+0.41, +0.90]$	$[+0.18, +1.16]$	2.8σ
C_{10}'	-0.05	$[-0.22, +0.11]$	$[-0.38, +0.28]$	0.3σ
$C_9^{\rm NP} = C_{10}^{\rm NP}$	-0.33	$[-0.53, -0.12]$	$[-0.70, +0.13]$	1.5σ
$C_9^{\rm NP} = -C_{10}^{\rm NP}$	-0.61	$[-0.74, -0.45]$	$[-0.92, -0.31]$	4.3σ
$C_9' = C_{10}'$	$+0.07$	$[-0.18, +0.32]$	$[-0.44, +0.58]$	0.3σ
$C_9' = -C_{10}'$	$+0.05$	$[-0.05, +0.15]$	$[-0.15, +0.25]$	0.5σ
$C_9^{\rm NP}, C_{10}^{\rm NP}$	$(-1.17, +0.16)$	—	—	4.6σ
$C_9^{\rm NP}, C_9'$	$(-1.25, +0.55)$	—	—	4.9σ
$C_9^{\rm NP}, C_{10}'$	$(-1.34, -0.36)$	—	—	5.0σ
$C_9', C_{10}^{\rm NP}$	$(+0.17, +0.66)$	—	—	2.4σ
C_9', C_{10}'	$(+0.18, +0.05)$	—	—	0.2σ
$C_{10}^{\rm NP}, C_{10}'$	$(+0.64, -0.01)$	—	—	2.4σ

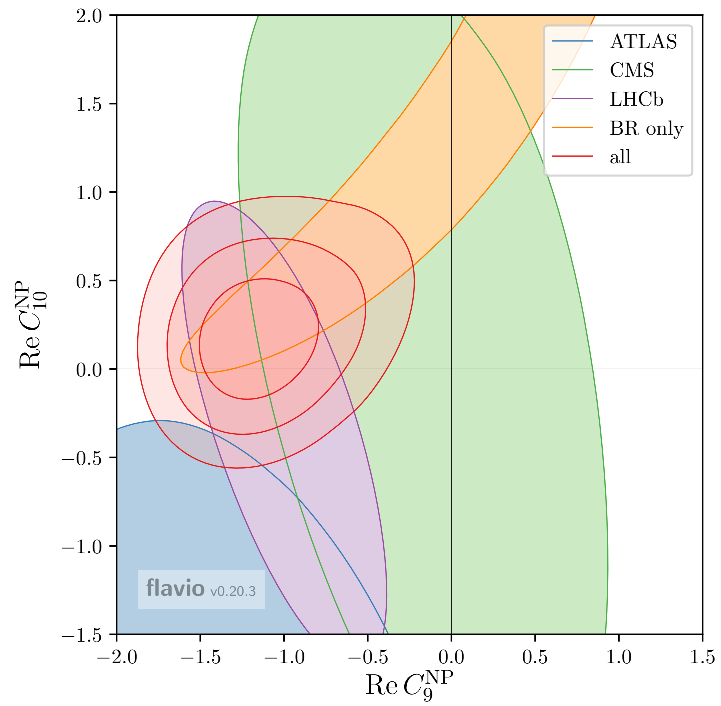

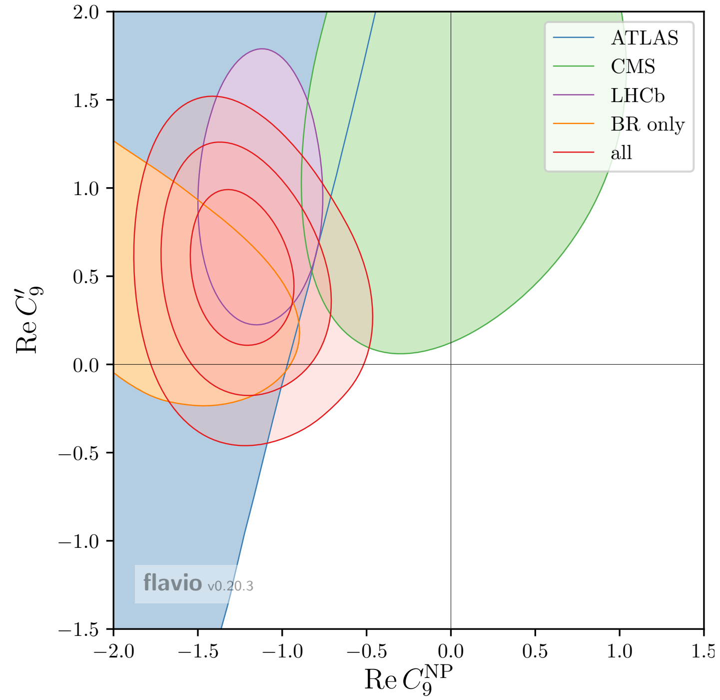

- The data can be described by NP in C_9^μ.

1D fits

Capdevila, Crivellin, Descotes-Genon, Matias & Virto, 1704.05340

- A NP contribution to muons is strongly preferred to that in electrons due to the angular data in $B \to K^* \mu\mu$.

	All			$[\sigma]$	$[\%]$	LFUV			$[\sigma]$	$[\%]$
1D Hyp.	Best fit	$1\ \sigma$	$2\ \sigma$	$\mathrm{Pull}_{\mathrm{SM}}$	p-value	Best fit	$1\ \sigma$	$2\ \sigma$	$\mathrm{Pull}_{\mathrm{SM}}$	p-value
$\mathcal{C}_{9\mu}^{\mathrm{NP}}$	-1.10	$[-1.27, -0.92]$	$[-1.43, -0.74]$	5.7	72	-1.76	$[-2.36, -1.23]$	$[-3.04, -0.76]$	3.9	69
$\mathcal{C}_{9\mu}^{\mathrm{NP}} = -\mathcal{C}_{10\mu}^{\mathrm{NP}}$	-0.61	$[-0.73, -0.48]$	$[-0.87, -0.36]$	5.2	61	-0.66	$[-0.84, -0.48]$	$[-1.04, -0.32]$	4.1	78
$\mathcal{C}_{9\mu}^{\mathrm{NP}} = -\mathcal{C}'_{9\mu}$	-1.01	$[-1.18, -0.84]$	$[-1.33, -0.65]$	5.4	66	-1.64	$[-2.12, -1.05]$	$[-2.52, -0.49]$	3.2	31
$\mathcal{C}_{9\mu}^{\mathrm{NP}} = -3\mathcal{C}_{9e}^{\mathrm{NP}}$	-1.06	[-1.23,-0.89]	[-1.39,-0.71]	5.8	74	-1.35	$[-1.82, -0.95]$	$[-2.38, -0.59]$	4.0	71

$$C_{9\mu}^{\mathrm{NP}} < 0 \qquad |C_{9\mu}^{\mathrm{NP}}/C_{9\mu}^{\mathrm{SM}}| \sim 25\,\%$$

- The 3rd hypothesis that would fail to explain R_K are not disfavored due to their good compatibility with R_{K^*} data.

Signs of NP contributions to coefficients

		R_K	$\langle P_5' \rangle_{[4,6],[6,8]}$	$\mathcal{B}_{B_s \to \phi\mu\mu}$
$\mathcal{C}_9^{\mathrm{NP}}$	$+$			
	$-$	✓	✓	✓
$\mathcal{C}_{10}^{\mathrm{NP}}$	$+$	✓		✓
	$-$		✓	
$\mathcal{C}_{9'}^{\mathrm{NP}}$	$+$			✓
	$-$	✓	✓	
$\mathcal{C}_{10'}^{\mathrm{NP}}$	$+$	✓	✓	
	$-$			✓

Descotes-Genon, et al., arXiv:1510.04239

$$O_9 = (\bar{s}\gamma_\mu P_L b)(\bar{\ell}\gamma^\mu \ell)\,,$$
$$O_{10} = (\bar{s}\gamma_\mu P_L b)(\bar{\ell}\gamma^\mu \gamma_5 \ell)\,,$$
$$O_9' = (\bar{s}\gamma_\mu P_R b)(\bar{\ell}\gamma^\mu \ell)\,,$$
$$O_{10}' = (\bar{s}\gamma_\mu P_R b)(\bar{\ell}\gamma^\mu \gamma_5 \ell)\,,$$

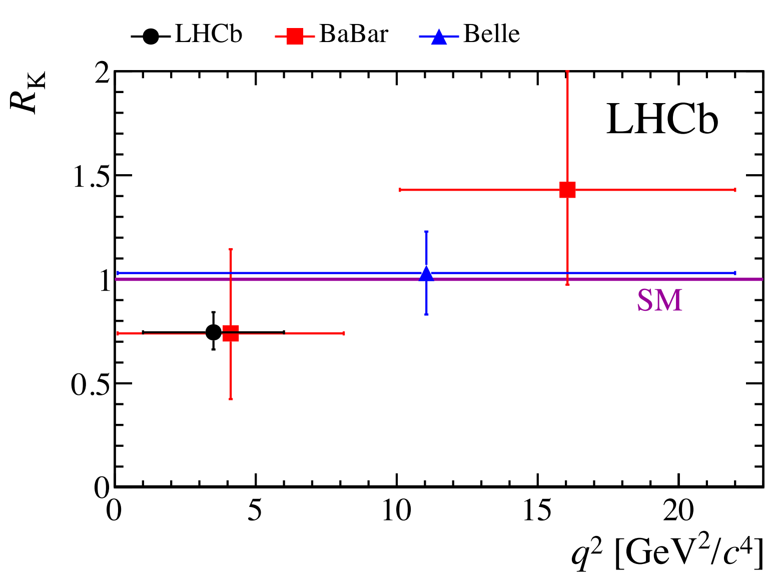

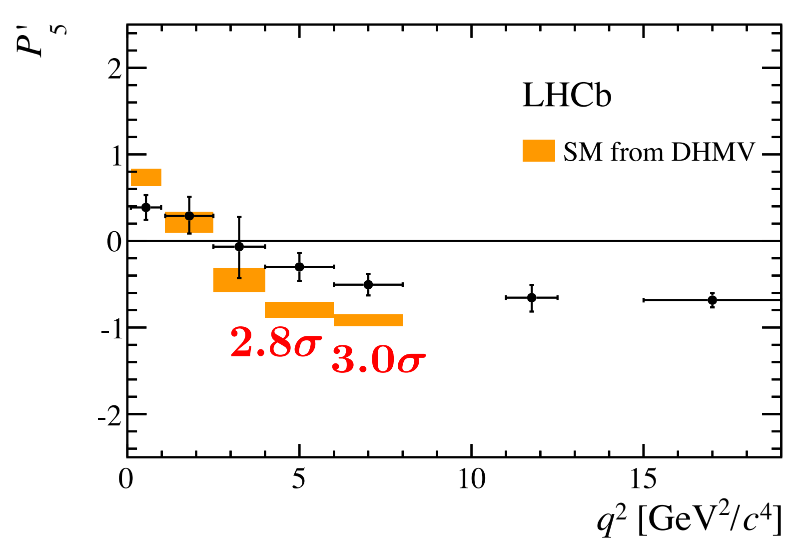

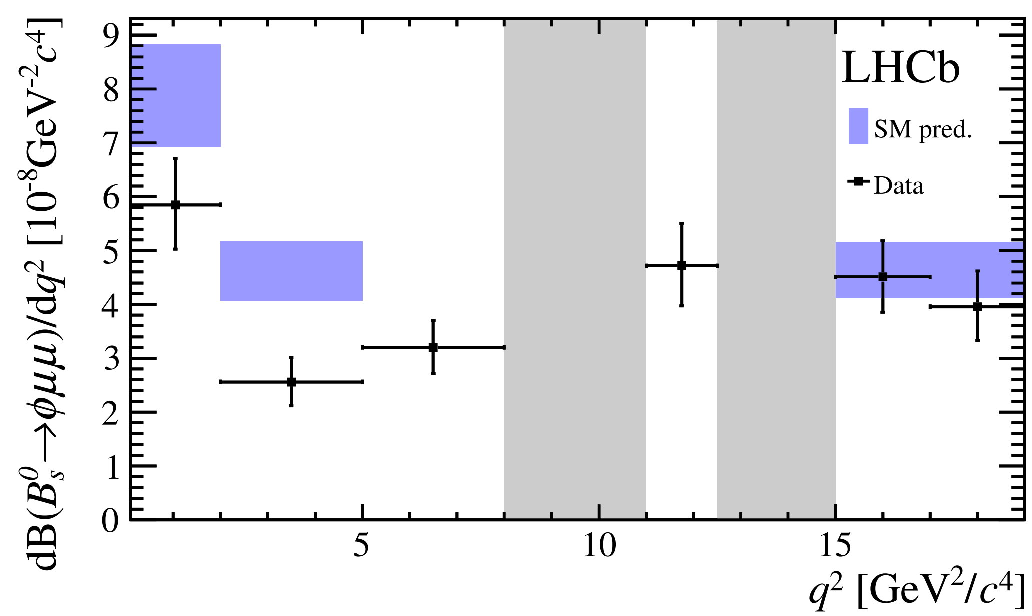

NP shifts in angular observables

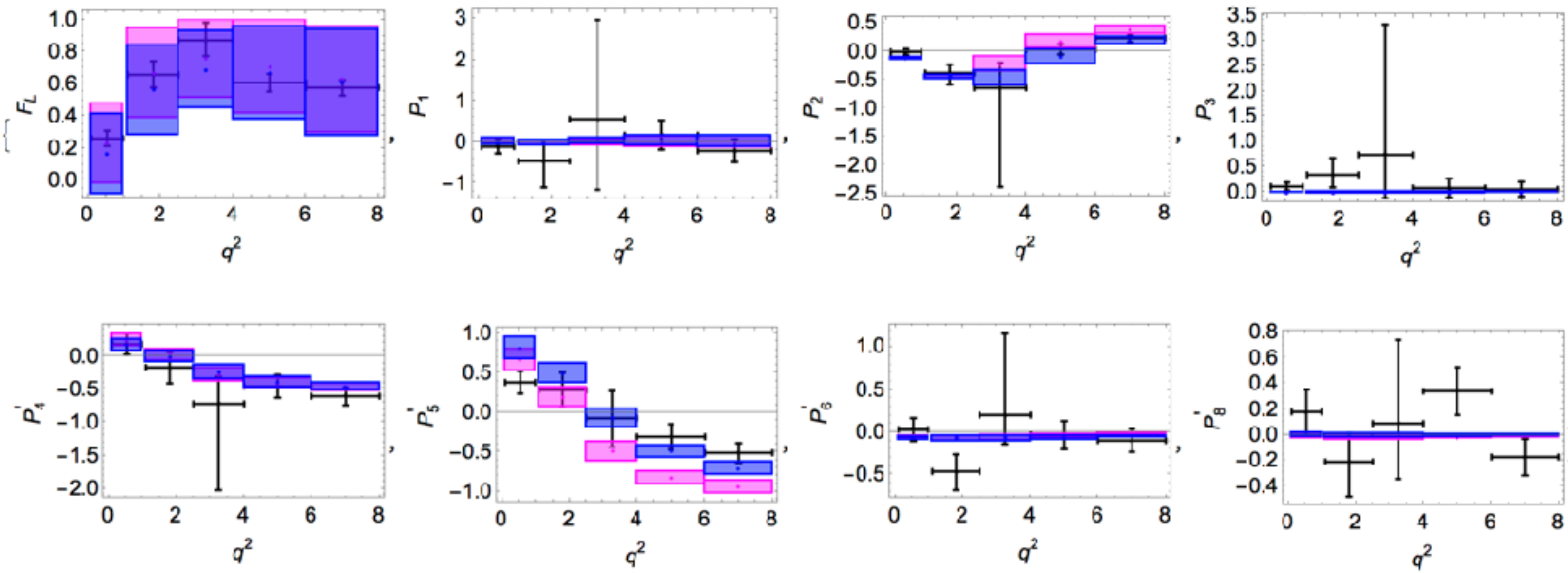

Pink: SM

Blue: NP with $C_{9\mu}^{\mathrm{NP}} = -1.3$

Capdevila, Crivellin, Descotes-Genon, Matias & Virto, 1704.05340

2D fits

- NP in C_9^μ ?

2D Hyp.	All: Best fit	All: $\mathrm{Pull_{SM}}$	All: p-value	LFUV: Best fit	LFUV: $\mathrm{Pull_{SM}}$	LFUV: p-value
$(\mathcal{C}_{9\mu}^{\rm NP},\mathcal{C}_{10\mu}^{\rm NP})$	(-1.17,0.15)	5.5	74	(-1.13,0.40)	3.7	75
$(\mathcal{C}_{9\mu}^{\rm NP},\mathcal{C}_{7}')$	(-1.05,0.02)	5.5	73	(-1.75,-0.04)	3.6	66
$(\mathcal{C}_{9\mu}^{\rm NP},\mathcal{C}_{9'\mu})$	(-1.09,0.45)	5.6	75	(-2.11,0.83)	3.7	73
$(\mathcal{C}_{9\mu}^{\rm NP},\mathcal{C}_{10'\mu})$	(-1.10,-0.19)	5.6	76	(-2.43,-0.54)	3.9	85
$(\mathcal{C}_{9\mu}^{\rm NP},\mathcal{C}_{9e}^{\rm NP})$	(-0.97,0.50)	5.4	72	(-1.09,0.66)	3.5	65

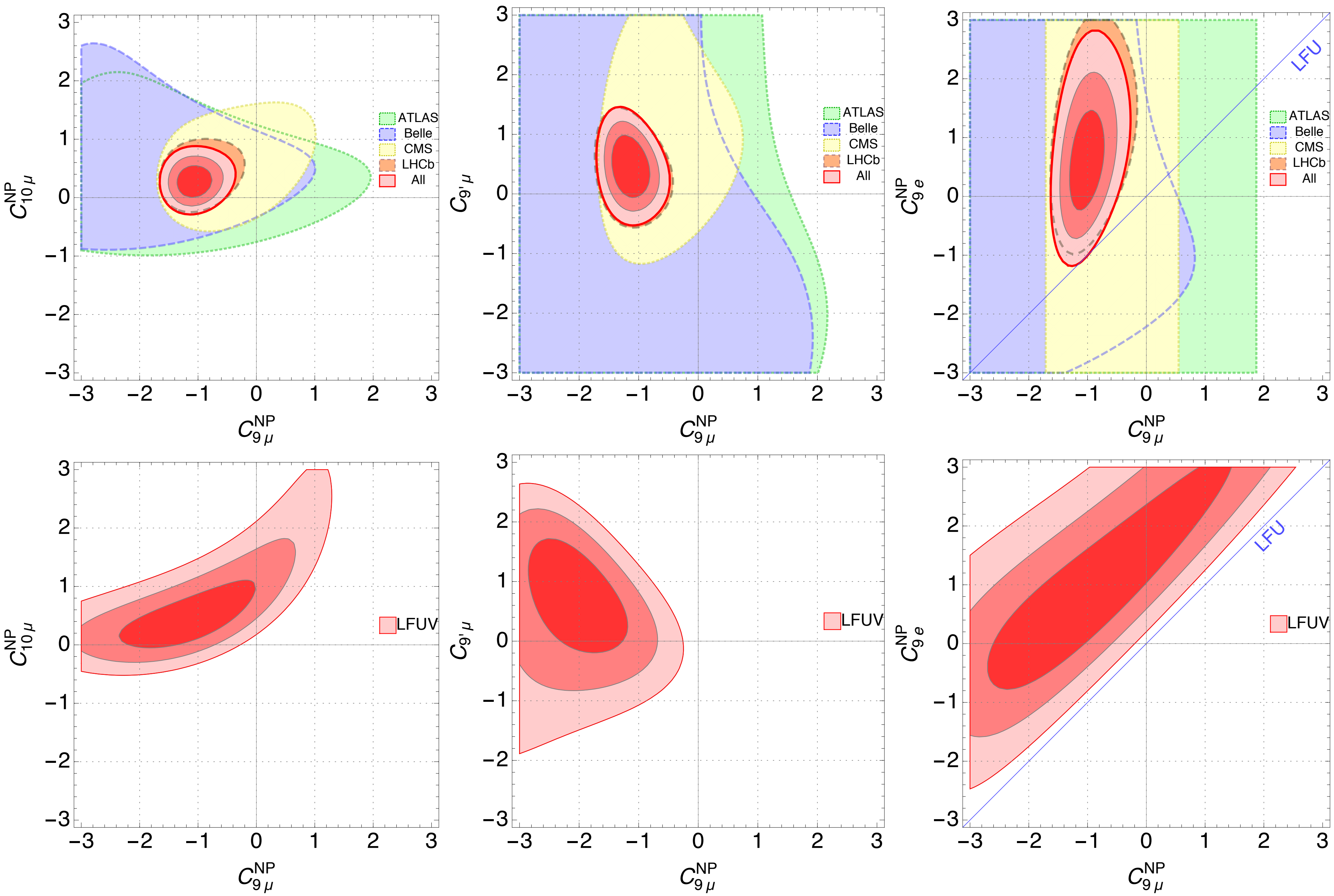

Satoshi Mishima (KEK)

2D fits by another group

Altmannshofer, Stangl & Straub, 1704.05435

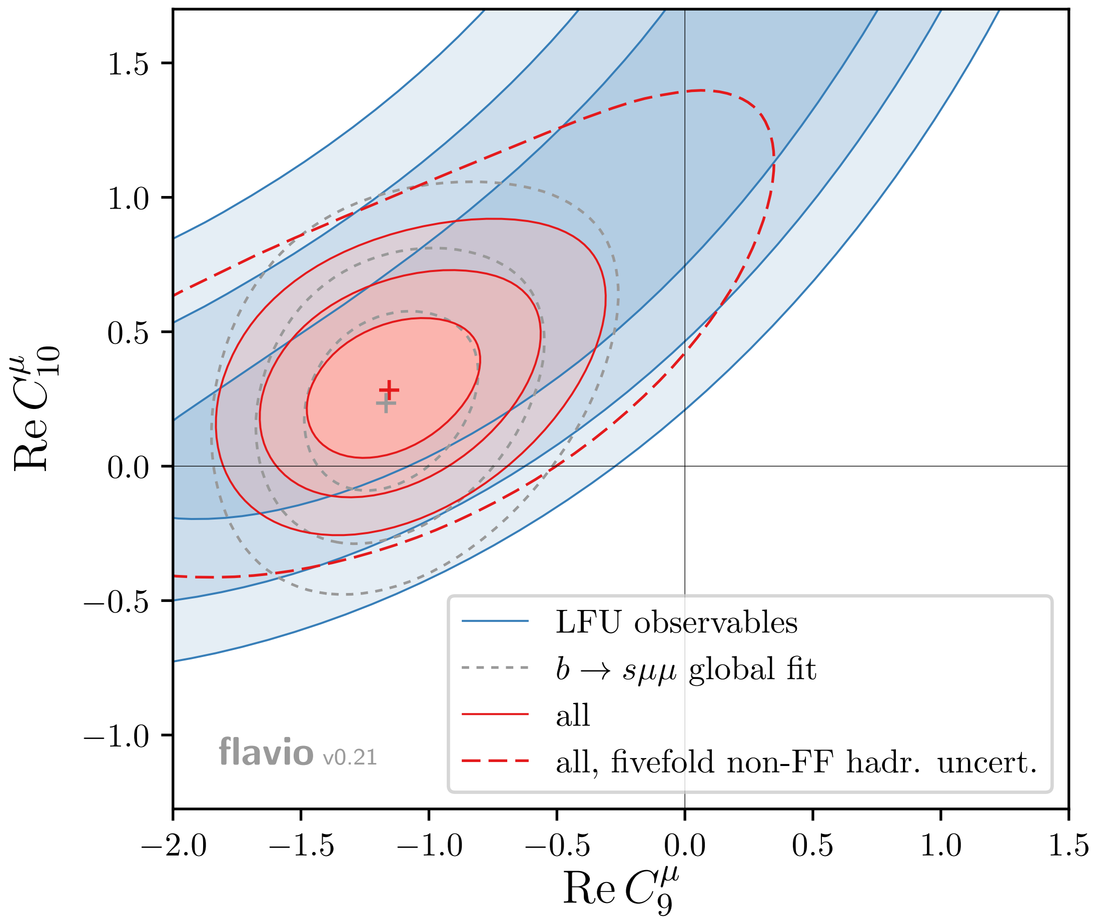

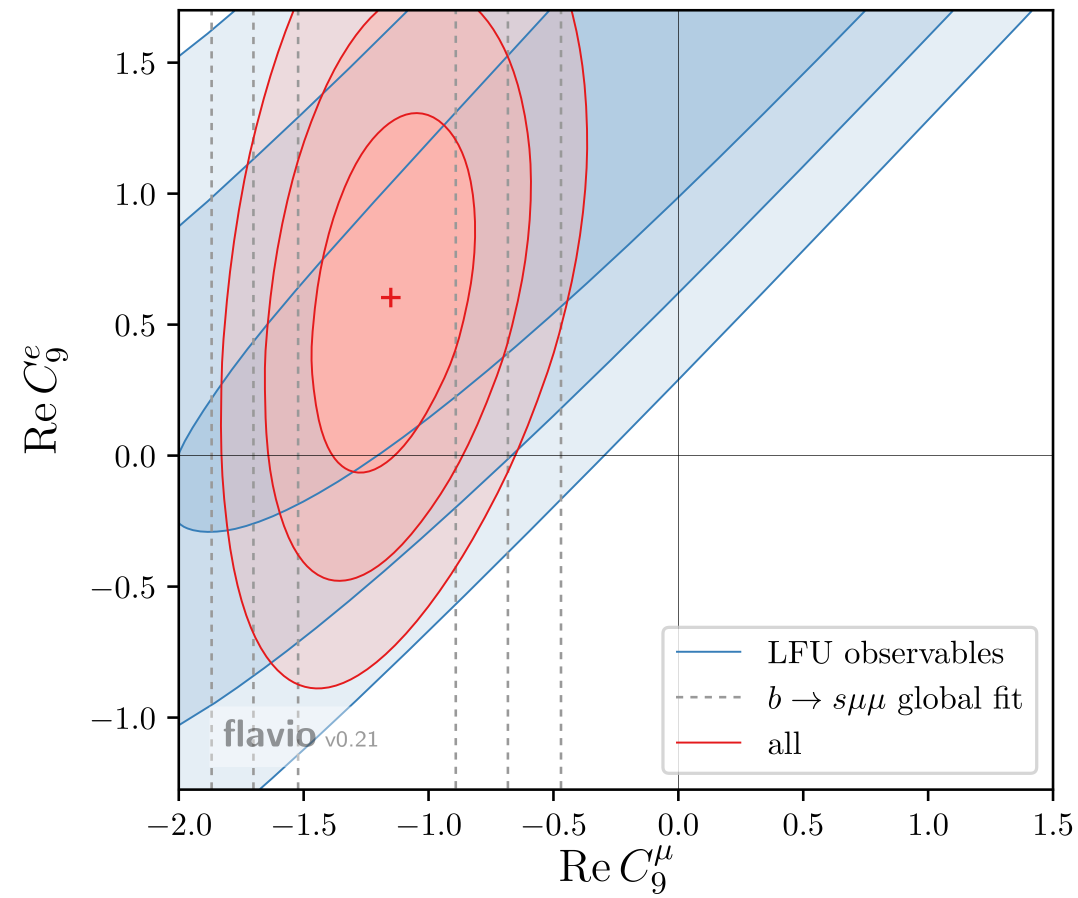

- The results are very similar to those by Capdevila et al.
- In the left plot, uncertainties of hadronic contributions are inflated by a factor of 5 w.r.t. their nominal estimates.

6D fit

Capdevila, Crivellin, Descotes-Genon, Matias & Virto, 1704.05340

	$\mathcal{C}_7^{\rm NP}$	$\mathcal{C}_{9\mu}^{\rm NP}$	$\mathcal{C}_{10\mu}^{\rm NP}$	$\mathcal{C}_{7'}$	$\mathcal{C}_{9'\mu}$	$\mathcal{C}_{10'\mu}$
Best fit	+0.017	-1.12	+0.33	+0.03	+0.59	+0.07
1 σ	$[-0.01, +0.05]$	$[-1.34, -0.85]$	$[+0.09, +0.59]$	$[+0.00, +0.06]$	$[+0.01, +1.12]$	$[-0.23, +0.37]$
2 σ	$[-0.03, +0.07]$	$[-1.51, -0.61]$	$[-0.10, +0.80]$	$[-0.02, +0.08]$	$[-0.50, +1.56]$	$[-0.50, +0.64]$

- 6D fit to "All" data
- SM pull: ~5 sigma

$$\mathcal{C}_7^{\rm NP} \gtrsim 0,\ \mathcal{C}_{9\mu}^{\rm NP} < 0,\ \mathcal{C}_{10\mu}^{\rm NP} > 0,\ \mathcal{C}_7' \gtrsim 0,\ \mathcal{C}_{9\mu}' > 0,\ \mathcal{C}_{10\mu}' \gtrsim 0$$

where $\mathcal{C}_{9\mu}$ is compatible with the SM beyond 3 σ, $\mathcal{C}_{10\mu}$, $\mathcal{C}_{7'}$ and $\mathcal{C}_{9'}$ at 2 σ and all the other coefficients at 1 σ.

- The result confirms the need for a large negative contribution to C_9^{μ}.

Fit of LL, LR, RL, RR, …

D'Amico, et al., 1704.05438

Wilson coeff.	Best-fit 'clean'	Best-fit 'dirty'	Best-fit all	1-σ range 'clean'	1-σ range 'dirty'	1-σ range all	$\sqrt{\chi^2_{\rm SM}-\chi^2_{\rm best}}$ 'clean'	$\sqrt{\chi^2_{\rm SM}-\chi^2_{\rm best}}$ 'dirty'	$\sqrt{\chi^2_{\rm SM}-\chi^2_{\rm best}}$ all
New physics in the muon sector									
$C^{\rm BSM}_{b_L\mu_L}$	-1.33	-1.33	-1.33	-0.99 -1.70	-1.01 -1.68	-1.10 -1.58	4.1	4.6	6.2
$C^{\rm BSM}_{b_L\mu_R}$	0.68	-0.73	-0.35	1.27 0.10	-0.40 -1.03	-0.03 -0.65	1.2	2.1	1.1
$C^{\rm BSM}_{b_R\mu_L}$	0.03	-0.20	-0.15	0.32 -0.26	-0.04 -0.29	-0.01 -0.25	0.1	1.3	1.1
$C^{\rm BSM}_{b_R\mu_R}$	-0.44	0.41	0.29	0.14 -1.00	0.61 0.18	0.50 0.07	0.8	1.7	1.3
New physics in the electron sector									
$C^{\rm BSM}_{b_Le_L}$	1.72	0.15	0.99	2.31 1.21	0.69 -0.39	1.30 0.70	4.1	0.3	3.5
$C^{\rm BSM}_{b_Le_R}$	-5.15	-1.70	-3.46	-4.23 -6.10	0.33 -2.83	-2.81 -4.05	4.3	0.9	3.6
$C^{\rm BSM}_{b_Re_L}$	0.085	-0.51	0.02	0.39 -0.21	0.29 -1.55	0.30 -0.25	0.3	0.7	0.1
$C^{\rm BSM}_{b_Re_R}$	-5.60	2.10	-3.63	-4.66 -6.56	3.52 -2.70	-2.65 -4.43	4.2	0.5	2.5

clean: $R_{K^{(*)}}, \cdots$

dirty: angular obs', …

larger NP contributions

- "dirty" obs' favor a deviation from the SM in the same directions as "clean" ones.
- $C^{\rm BSM}_{b_L\mu_L} < 0$

More results

D'Amico, et al., 1704.05438

4D fit

$$
\begin{aligned}
C^{\rm BSM}_{b_L\mu_L} &= -1.35 \pm 0.22 \\
C^{\rm BSM}_{b_R\mu_L} &= +0.44 \pm 0.21 \\
C^{\rm BSM}_{b_L\mu_R} &= -0.33 \pm 0.33 \\
C^{\rm BSM}_{b_R\mu_R} &= +0.86 \pm 0.54
\end{aligned}
\qquad \text{with} \qquad
\rho = \begin{pmatrix} 1 & -0.26 & 0.02 & -0.33 \\ -0.26 & 1 & -0.17 & 0.47 \\ 0.02 & -0.17 & 1 & 0.25 \\ -0.33 & 0.47 & 0.25 & 1 \end{pmatrix}
$$

electron vs. muon

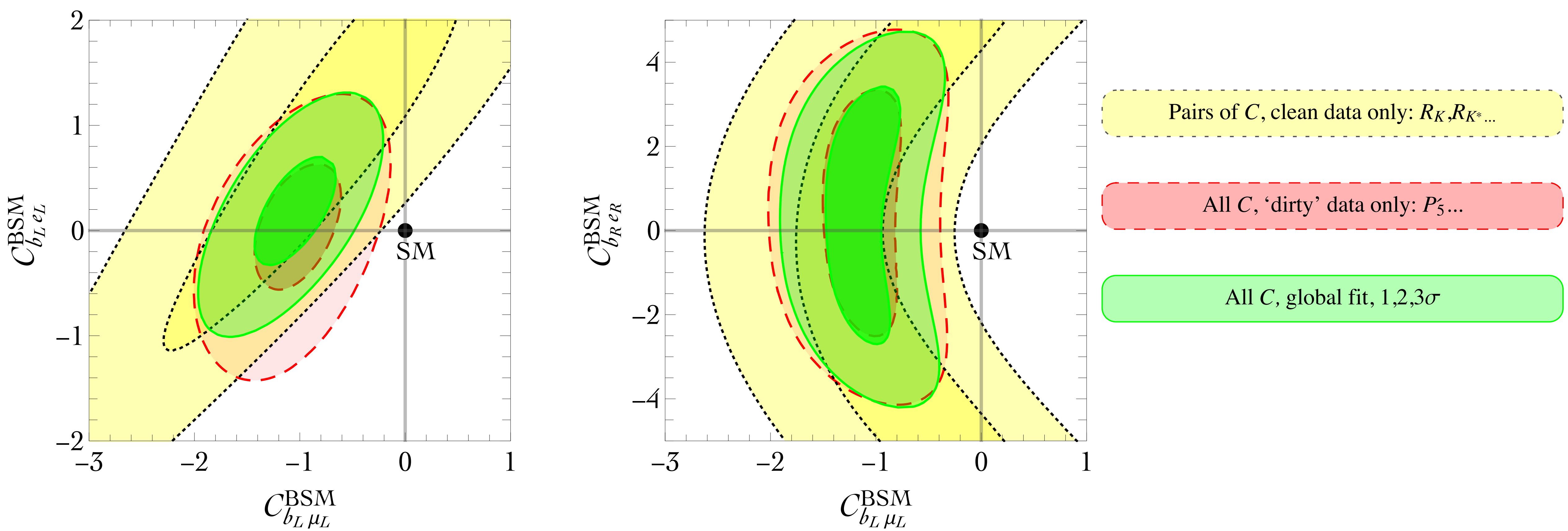

Global Bayesian 8D fit

D'Amico, et al., 1704.05438

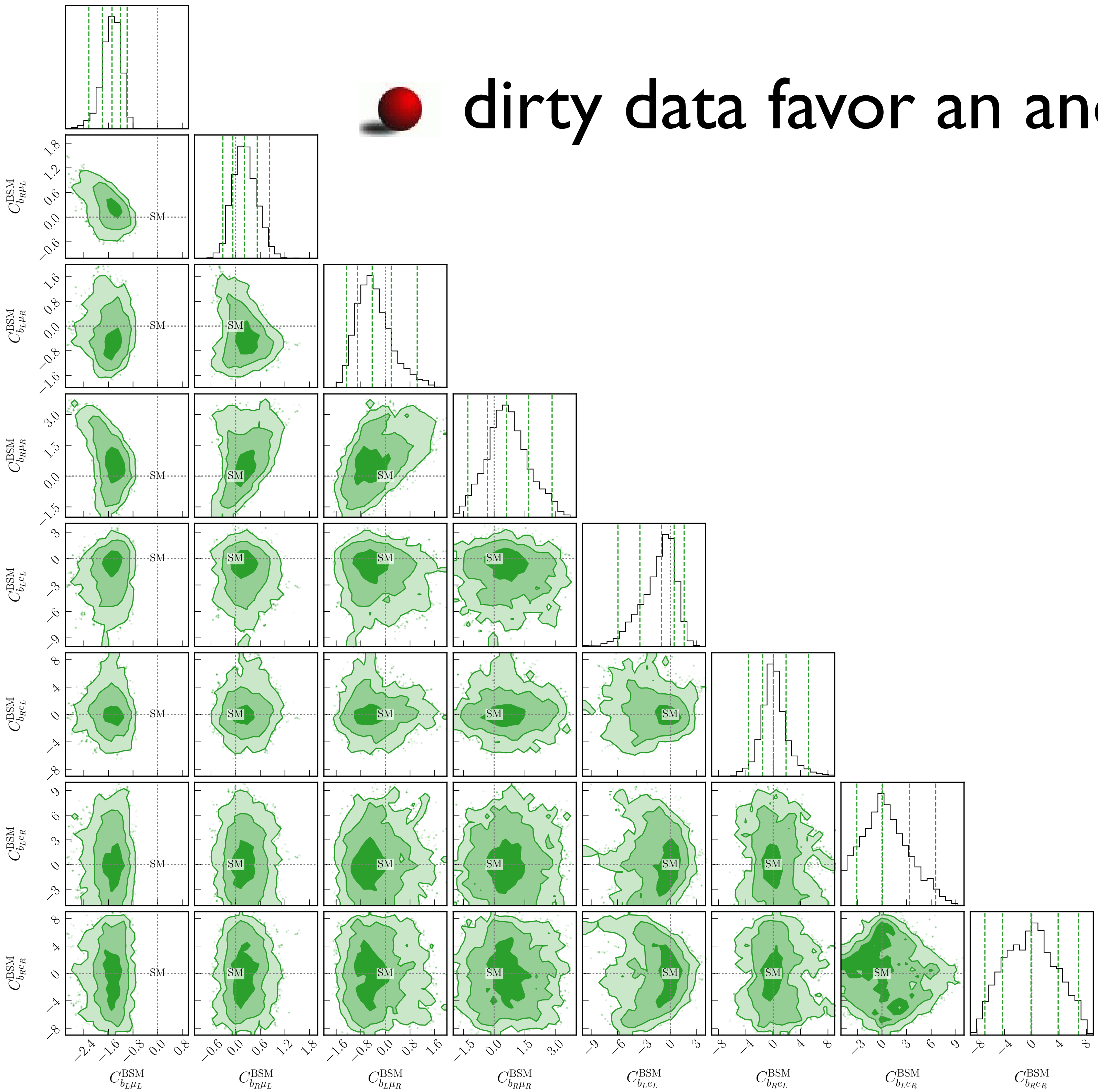

- dirty data favor an anomaly in muons.

Implication to NP scale

W. Almannshofer, Talk at Aspen, Jan. 2016

generic tree	$\frac{1}{\Lambda_{\mathrm{NP}}^2}(\bar{s}\gamma_\nu P_L b)(\bar{\mu}\gamma^\nu \mu)$	$\Lambda_{\mathrm{NP}} \simeq 35\ \mathrm{TeV} \times (C_9^{\mathrm{NP}})^{-1/2}$
MFV tree	$\frac{1}{\Lambda_{\mathrm{NP}}^2}\ V_{tb}V_{ts}^*\ (\bar{s}\gamma_\nu P_L b)(\bar{\mu}\gamma^\nu \mu)$	$\Lambda_{\mathrm{NP}} \simeq 7\ \mathrm{TeV} \times (C_9^{\mathrm{NP}})^{-1/2}$
generic loop	$\frac{1}{\Lambda_{\mathrm{NP}}^2}\frac{1}{16\pi^2}(\bar{s}\gamma_\nu P_L b)(\bar{\mu}\gamma^\nu \mu)$	$\Lambda_{\mathrm{NP}} \simeq 3\ \mathrm{TeV} \times (C_9^{\mathrm{NP}})^{-1/2}$
MFV loop	$\frac{1}{\Lambda_{\mathrm{NP}}^2}\frac{1}{16\pi^2}\ V_{tb}V_{ts}^*\ (\bar{s}\gamma_\nu P_L b)(\bar{\mu}\gamma^\nu \mu)$	$\Lambda_{\mathrm{NP}} \simeq 0.6\ \mathrm{TeV} \times (C_9^{\mathrm{NP}})^{-1/2}$

NP or hadronic effects?

- NP contributions are independent of q2 and universal for all helicity amplitudes.

Altmannshofer, Niehoff, Stangl & Straub, 1703.09189

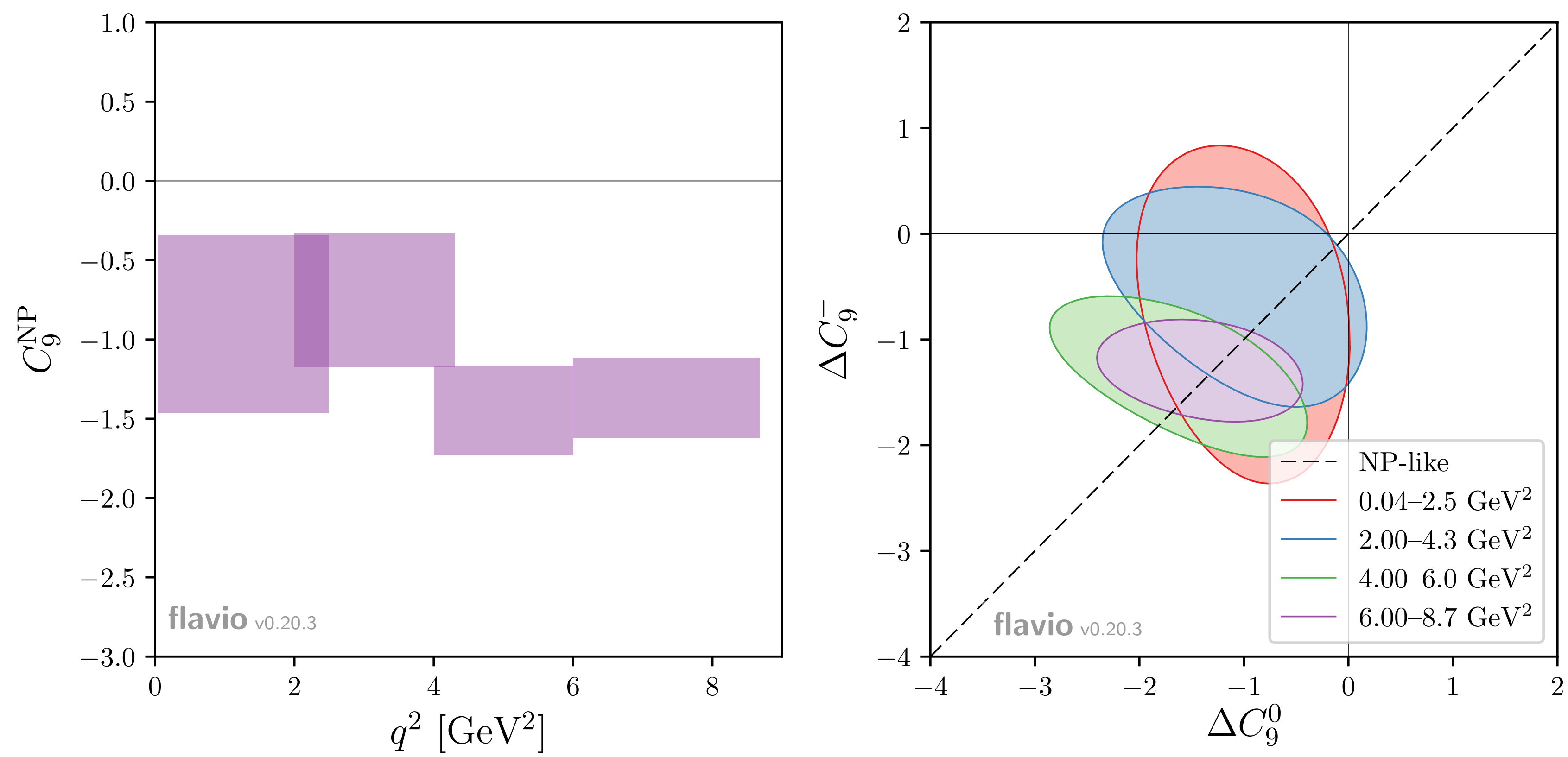

- compatible with a flat q2 dependence.
- consistent with a universal effect in different polarizations.
- but cannot exclude a possibility of large hadronic effects.

NP or hadronic effects?

- Hadronic contributions have been taken as fitting parameters:

Ciuchini et al., 1704.05447

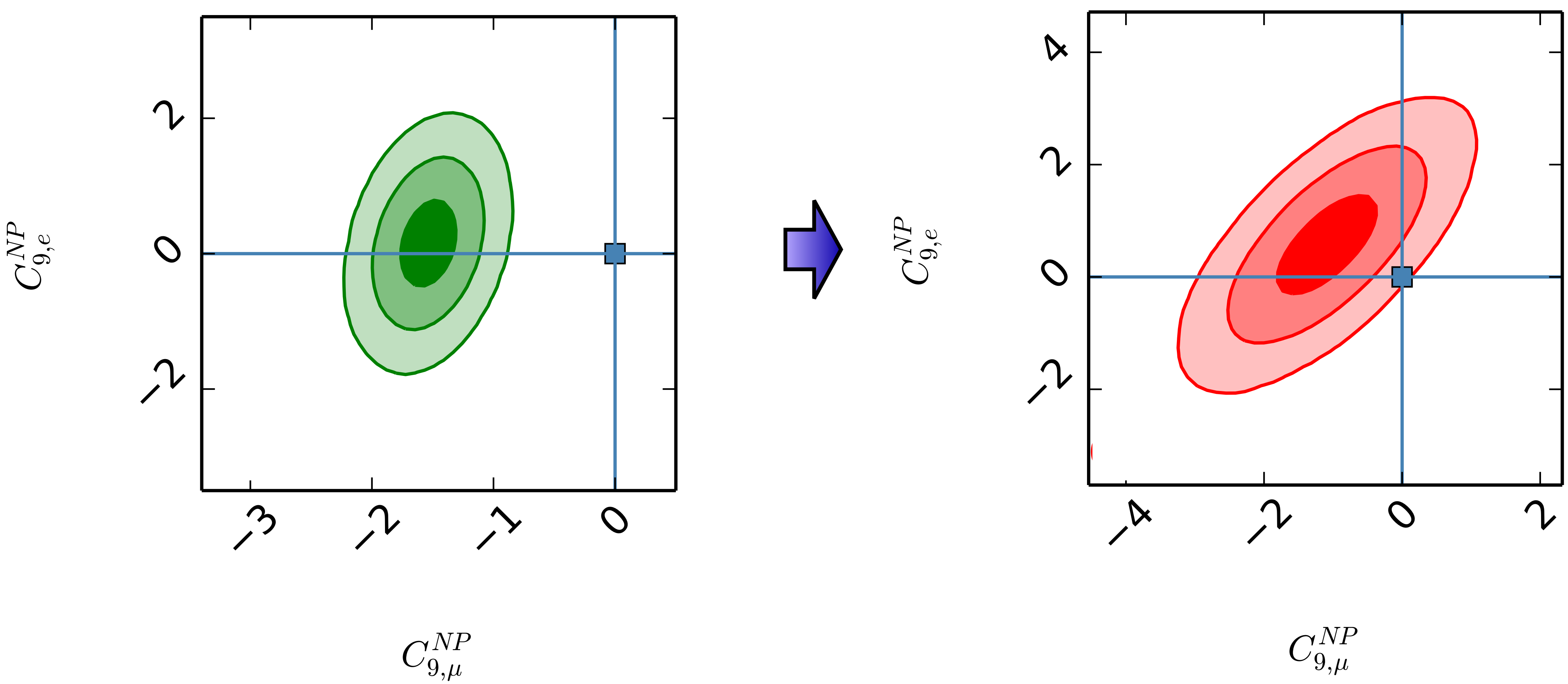

C9 vs. C10 and electron vs. muon

$$Q_{4,5} = P'^{\mu}_{4,5} - P'^{e}_{4,5}$$

Q_4

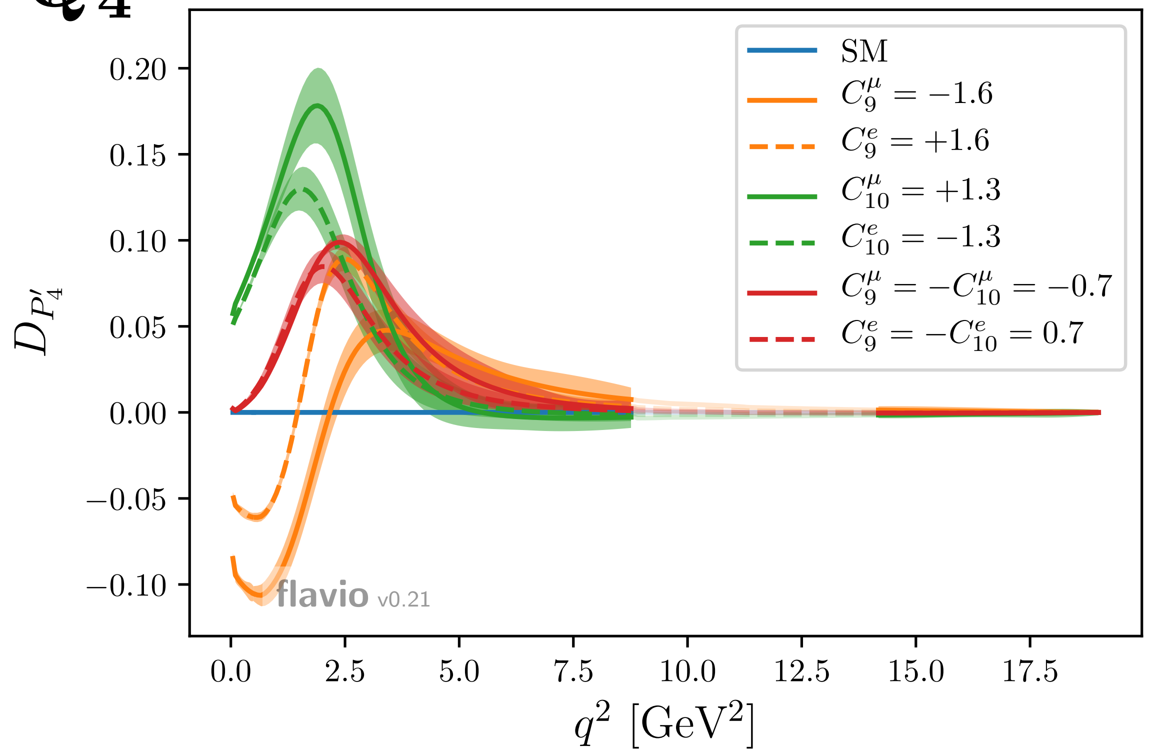

Q_5

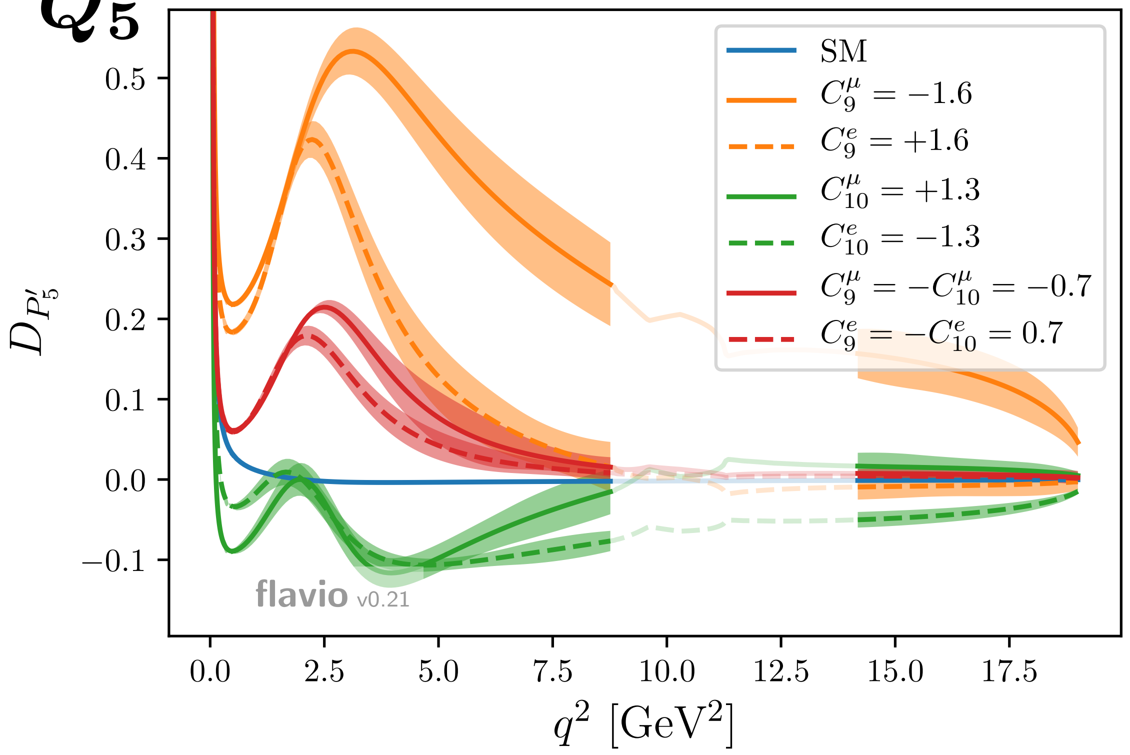

- $Q_{4,5}$ will be very powerful tools to lift degeneracies in the fits.

Further observables

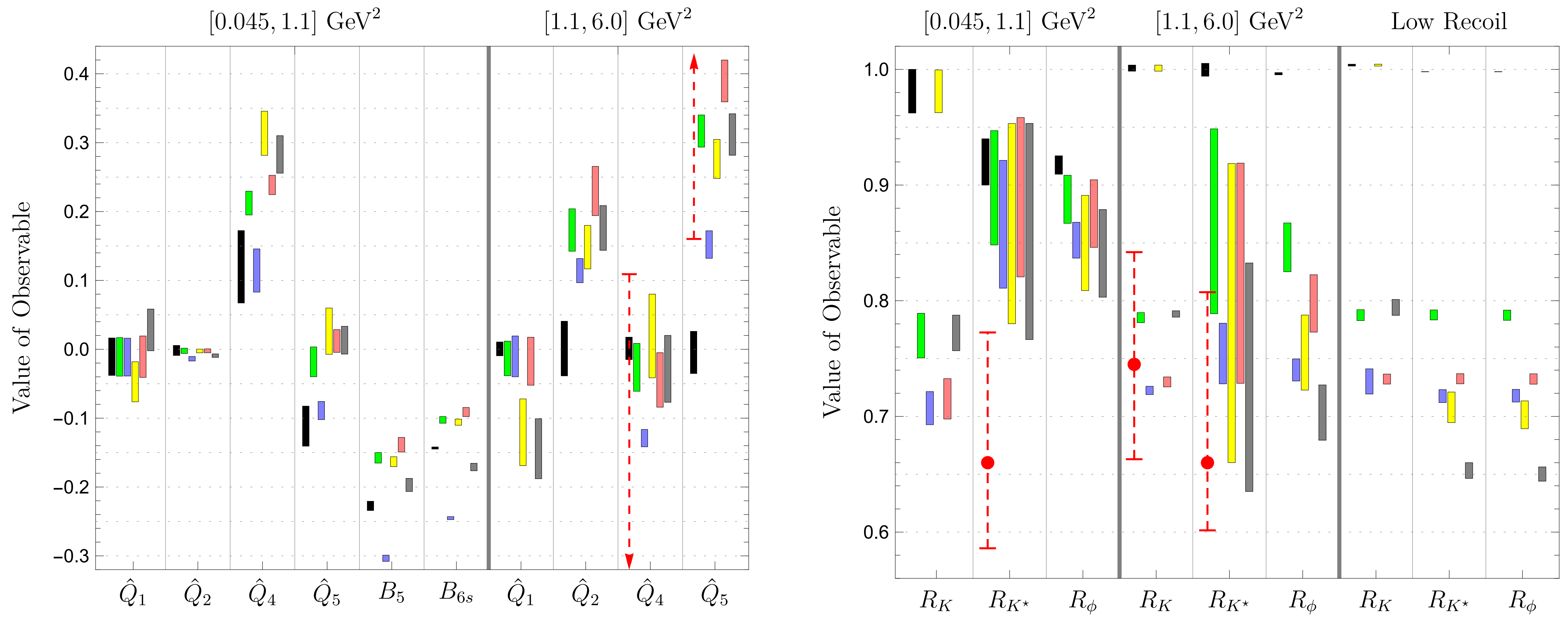

$$Q_i = P_i^\mu - P_i^e$$

$$B_i = \frac{J_i^\mu}{J_i^e} - 1$$

- ▶ Scenario 1: $C_{9\mu}^{\rm NP} = -1.1$,
- ▶ Scenario 2: $C_{9\mu}^{\rm NP} = -C_{10\mu}^{\rm NP} = -0.61$,
- ▶ Scenario 3: $C_{9\mu}^{\rm NP} = -C'_{9\mu} = -1.01$,
- ▶ Scenario 4: $C_{9\mu}^{\rm NP} = -3C_{9e}^{\rm NP} = -1.06$,
- ▶ Scenario 5: The best fit point in the six-dimensional fit (Table III).

SMEFT

- Experimental data suggest that the NP scale is well above the EW scale.
- Consider an EFT built exclusively from the SM fields with the SM gauge symmetries. $SU(3)_c \times SU(2)_L \times U(1)_Y$

$$\mathcal{L}_{\mathrm{SMEFT}} \supset \frac{1}{\Lambda^2} \sum_k \mathcal{C}_k Q_k \,.$$

$$\mathcal{C}_{9a}^{\mathrm{NP}} = \frac{\pi}{\alpha \lambda_t^{sb}} \frac{v^2}{\Lambda^2} \left\{ \left[\tilde{\mathcal{C}}_{\ell q}^{(1)}\right]_{aa23} + \left[\tilde{\mathcal{C}}_{\ell q}^{(3)}\right]_{aa23} + \left[\tilde{\mathcal{C}}_{qe}\right]_{23aa} \right\},$$

$$\mathcal{C}_{10a}^{\mathrm{NP}} = -\frac{\pi}{\alpha \lambda_t^{sb}} \frac{v^2}{\Lambda^2} \left\{ \left[\tilde{\mathcal{C}}_{\ell q}^{(1)}\right]_{aa23} + \left[\tilde{\mathcal{C}}_{\ell q}^{(3)}\right]_{aa23} - \left[\tilde{\mathcal{C}}_{qe}\right]_{23aa} \right\},$$

$$\mathcal{C}_{9a}^{\prime} = \frac{\pi}{\alpha \lambda_t^{sb}} \frac{v^2}{\Lambda^2} \left\{ \left[\tilde{\mathcal{C}}_{\ell d}\right]_{aa23} + \left[\tilde{\mathcal{C}}_{ed}\right]_{aa23} \right\},$$

$$\mathcal{C}_{10a}^{\prime} = -\frac{\pi}{\alpha \lambda_t^{sb}} \frac{v^2}{\Lambda^2} \left\{ \left[\tilde{\mathcal{C}}_{\ell d}\right]_{aa23} - \left[\tilde{\mathcal{C}}_{ed}\right]_{aa23} \right\}.$$

Celis, Fuentes-Martin, Vicente & Virto, 1704.05672

SMEFT operator	Definition	Matching	Order
$[Q_{\ell q}^{(1)}]_{aa23}$	$(\bar{\ell}_a \gamma_\mu \ell_a)\,(\bar{q}_2 \gamma^\mu q_3)$	$\mathcal{O}_{9,10}$	Tree
$[Q_{\ell q}^{(3)}]_{aa23}$	$(\bar{\ell}_a \gamma_\mu \tau^I \ell_a)\,(\bar{q}_2 \gamma^\mu \tau^I q_3)$	$\mathcal{O}_{9,10}$	Tree
$[Q_{qe}]_{23aa}$	$(\bar{q}_2 \gamma_\mu q_3)\,(\bar{e}_a \gamma^\mu e_a)$	$\mathcal{O}_{9,10}$	Tree
$[Q_{\ell d}]_{aa23}$	$(\bar{\ell}_a \gamma_\mu \ell_a)\,(\bar{d}_2 \gamma^\mu d_3)$	$\mathcal{O}_{9,10}^{\prime}$	Tree
$[Q_{ed}]_{aa23}$	$(\bar{e}_a \gamma_\mu e_a)\,(\bar{d}_2 \gamma^\mu d_3)$	$\mathcal{O}_{9,10}^{\prime}$	Tree
$[Q_{\varphi \ell}^{(1)}]_{aa}$	$(\varphi^\dagger i \overleftrightarrow{D}_\mu \varphi)\,(\bar{\ell}_a \gamma^\mu \ell_a)$	$\mathcal{O}_{9,10}$	1-loop
$[Q_{\varphi \ell}^{(3)}]_{aa}$	$(\varphi^\dagger i \overleftrightarrow{D}_\mu^I \varphi)\,(\bar{\ell}_a \gamma^\mu \tau^I \ell_a)$	$\mathcal{O}_{9,10}$	1-loop
$[Q_{\ell u}]_{aa33}$	$(\bar{\ell}_a \gamma_\mu \ell_a)\,(\bar{u}_3 \gamma^\mu u_3)$	$\mathcal{O}_{9,10}$	1-loop
$[Q_{\varphi e}]_{aa}$	$(\varphi^\dagger i \overleftrightarrow{D}_\mu \varphi)\,(\bar{e}_a \gamma^\mu e_a)$	$\mathcal{O}_{9,10}$	1-loop
$[Q_{eu}]_{aa33}$	$(\bar{e}_a \gamma_\mu e_a)\,(\bar{u}_3 \gamma^\mu u_3)$	$\mathcal{O}_{9,10}$	1-loop

SMEFT

- $[\mathcal{C}_{\ell q}^{(1,3)}]_{2223}$ play a crucial role in the explanation of the anomalies

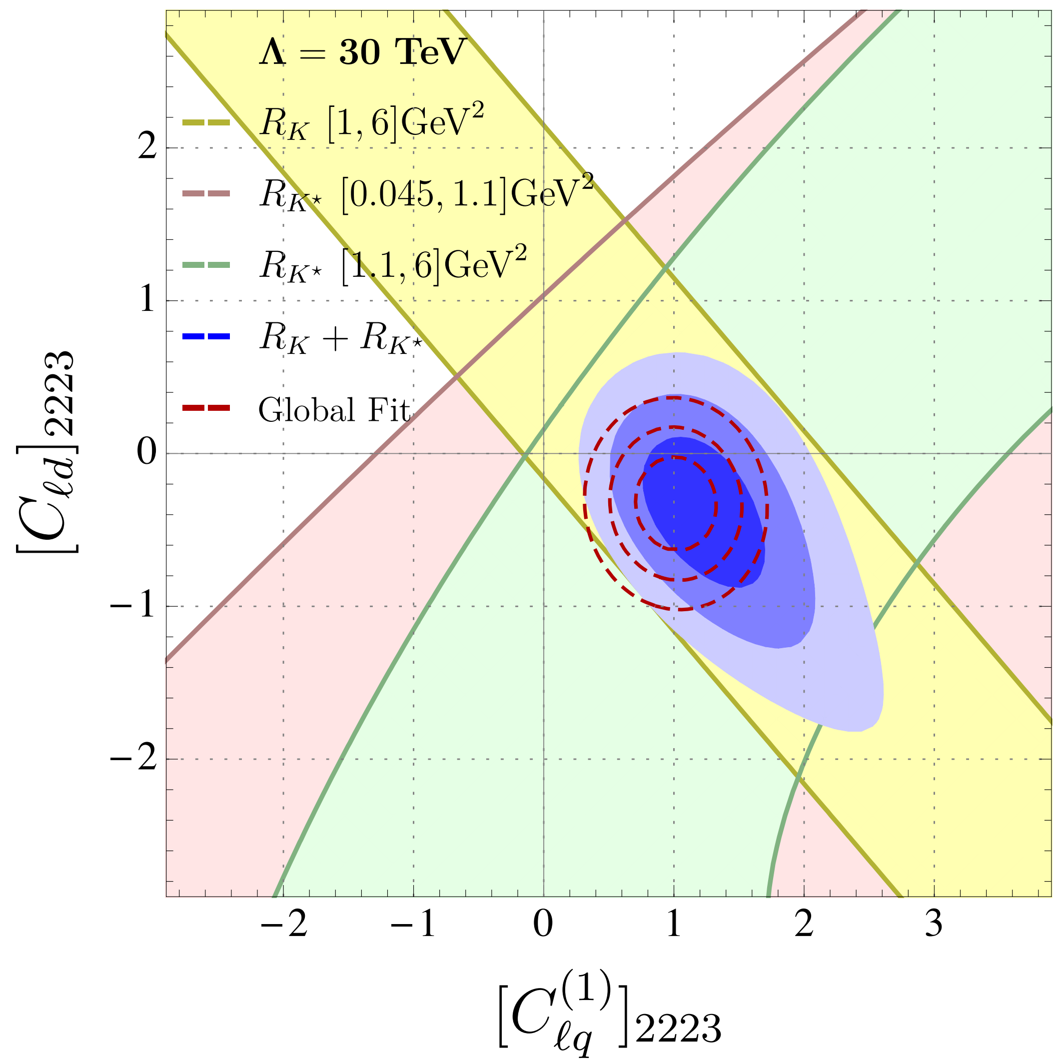

FIG. 2. Constraints on the SMEFT Wilson coefficients $\mathcal{C}_{\ell q}^{(1)}$ and $\mathcal{C}_{\ell d}$ with $\Lambda = 30$ TeV, assuming no NP in the electron modes. The individual constraints from R_K and R_{K^*} at the 3σ level are represented by filled bands. The combined fit to R_K and R_{K^*} is shown in blue (1,2 and 3 σ contours). The result of a global fit with all $b \to s\ell^+\ell^-$ data included in [7] is shown in a similar way as red dashed contours.

Celis, Fuentes-Martin, Vicente & Virto, 1704.05672
(see also Feruglio, Paradisi & Pattori, 1705.00929)

SMEFT operator	Definition	Matching	Order
$[Q_{\ell q}^{(1)}]_{aa23}$	$(\bar{\ell}_a\gamma_\mu\ell_a)\,(\bar{q}_2\gamma^\mu q_3)$	$\mathcal{O}_{9,10}$	Tree
$[Q_{\ell q}^{(3)}]_{aa23}$	$(\bar{\ell}_a\gamma_\mu\tau^I\ell_a)\,(\bar{q}_2\gamma^\mu\tau^I q_3)$	$\mathcal{O}_{9,10}$	Tree
$[Q_{qe}]_{23aa}$	$(\bar{q}_2\gamma_\mu q_3)\,(\bar{e}_a\gamma^\mu e_a)$	$\mathcal{O}_{9,10}$	Tree
$[Q_{\ell d}]_{aa23}$	$(\bar{\ell}_a\gamma_\mu\ell_a)\,(\bar{d}_2\gamma^\mu d_3)$	$\mathcal{O}'_{9,10}$	Tree
$[Q_{ed}]_{aa23}$	$(\bar{e}_a\gamma_\mu e_a)\,(\bar{d}_2\gamma^\mu d_3)$	$\mathcal{O}'_{9,10}$	Tree
$[Q_{\varphi\ell}^{(1)}]_{aa}$	$\left(\varphi^\dagger i\overleftrightarrow{D}_\mu\varphi\right)(\bar{\ell}_a\gamma^\mu\ell_a)$	$\mathcal{O}_{9,10}$	1-loop
$[Q_{\varphi\ell}^{(3)}]_{aa}$	$\left(\varphi^\dagger i\overleftrightarrow{D}^I_\mu\varphi\right)(\bar{\ell}_a\gamma^\mu\tau^I\ell_a)$	$\mathcal{O}_{9,10}$	1-loop
$[Q_{\ell u}]_{aa33}$	$(\bar{\ell}_a\gamma_\mu\ell_a)\,(\bar{u}_3\gamma^\mu u_3)$	$\mathcal{O}_{9,10}$	1-loop
$[Q_{\varphi e}]_{aa}$	$\left(\varphi^\dagger i\overleftrightarrow{D}_\mu\varphi\right)(\bar{e}_a\gamma^\mu e_a)$	$\mathcal{O}_{9,10}$	1-loop
$[Q_{eu}]_{aa33}$	$(\bar{e}_a\gamma_\mu e_a)\,(\bar{u}_3\gamma^\mu u_3)$	$\mathcal{O}_{9,10}$	1-loop

3. Summary

- RK and RK* can be explained by lepton-specific NP four-fermion contact interactions $(\bar{s}P_L b)(\bar{\ell}P_L\ell)$.

- Models with the RH quark current are disfavored, since they cannot explain RK<1 and RK*<1 simultaneously.

- LFUV and angular observables look consistent and favor independently the same pattern of deviations from the SM.

$$C_{9\mu}^{\mathrm{NP}} \approx -1.2 \qquad C_{b_L\mu_L}^{\mathrm{NP}} \approx -1.3$$

- Preferred hypotheses:

$$C_{9\mu}^{\mathrm{NP}}, \quad C_{9\mu}^{\mathrm{NP}} = -C_{10\mu}^{\mathrm{NP}}, \quad C_{9\mu}^{\mathrm{NP}} = C_{9\mu}^{\prime\mathrm{NP}}$$

- Future precise measurements of Q4 and Q5 can help to identify the chirality structure of the lepton currents.

Backup

Hadronic contributions

M. Ciuchini, M. Fedele, E. Franco, S.M. , A. Paul, L. Silvestrini & M. Valli, arXiv:1512.07157

- Hadronic contributions have been fitted from the data.

$$h_\lambda(q^2) = \frac{\epsilon^*_\mu(\lambda)}{m_B^2} \int d^4x e^{iqx} \langle \bar{K}^* | T\{j^\mu_{\rm em}(x) \mathcal{H}^{\rm had}_{\rm eff}(0)\} | \bar{B} \rangle$$
$$= h_\lambda^{(0)} + \frac{q^2}{1\,\mathrm{GeV}^2} h_\lambda^{(1)} + \frac{q^4}{1\,\mathrm{GeV}^4} h_\lambda^{(2)},$$

$$\tilde{g} \equiv \Delta C_9^{(\text{non pert.})}/(2C_1)$$

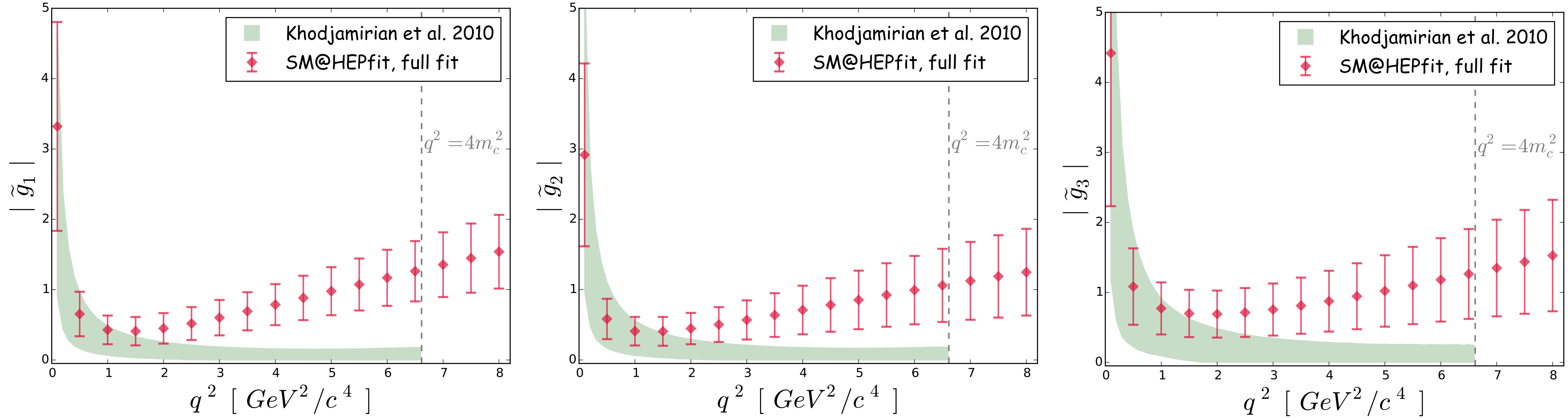

The hadronic cont's extracted from the data are compatible with the LCSR estimate for $q^2 \lesssim 1\ \mathbf{GeV^2}$ and seem to grow towards charm resonances.

- Not conclusive! Need more efforts!

See also 1701.08672, 1702.02234